Journal of Experimental Botany, Vol. 65, No. 13, pp. 3341–3356, 2014
doi:10.1093/jxb/eru180 Advance Access publication 12 May, 2014

Journal of Experimental Botany
www.jxb.oxfordjournals.org

REVIEW PAPER

From proto-Kranz to C_4 Kranz: building the bridge to C_4 photosynthesis

Rowan F. Sage, Roxana Khoshravesh and Tammy L. Sage*

Department of Ecology and Evolutionary Biology, The University of Toronto, 25 Willcocks Street, Toronto, On M5S3B2 Canada

* To whom correspondence should be addressed. E-mail: tammy.sage@utoronto.ca

Received 2 January 2014; Revised 14 March 2014; Accepted 24 March 2014

Abstract

In this review, we examine how the specialized "Kranz" anatomy of C_4 photosynthesis evolved from C_3 ancestors. Kranz anatomy refers to the wreath-like structural traits that compartmentalize the biochemistry of C_4 photosynthesis and enables the concentration of CO_2 around Rubisco. A simplified version of Kranz anatomy is also present in the species that utilize C_2 photosynthesis, where a photorespiratory glycine shuttle concentrates CO_2 into an inner bundle-sheath-like compartment surrounding the vascular tissue. C_2 Kranz is considered to be an intermediate stage in the evolutionary development of C_4 Kranz, based on the intermediate branching position of C_2 species in 14 evolutionary lineages of C_4 photosynthesis. In the best-supported model of C_4 evolution, Kranz anatomy in C_2 species evolved from C_3 ancestors with enlarged bundle sheath cells and high vein density. Four independent lineages have been identified where C_3 sister species of C_2 plants exhibit an increase in organelle numbers in the bundle sheath and enlarged bundle sheath cells. Notably, in all of these species, there is a pronounced shift of mitochondria to the inner bundle sheath wall, forming an incipient version of the C_2 type of Kranz anatomy. This incipient version of C_2 Kranz anatomy is termed proto-Kranz, and is proposed to scavenge photorespiratory CO_2. By doing so, it may provide fitness benefits in hot environments, and thus represent a critical first stage of the evolution of both the C_2 and C_4 forms of Kranz anatomy.

Key words: C_4 evolution, C_2 photosynthesis, C_4 photosynthesis, C_3–C_4 intermediate, glycine shuttle, Kranz anatomy, photorespiration, proto-Kranz anatomy.

Introduction

A major feature of C_4 photosynthesis is the specialization of leaf structure to form Kranz anatomy, wherein CO_2 is first assimilated by PEPcase in a layer of mesophyll (M) cells that surround an inner layer of bundle-sheath-like Kranz (K) cells, where CO_2 is concentrated and refixed by Rubisco (Fig. 1; Brown, 1975). Of the 65 to 70 known lineages of C_4 plants (Sage *et al.*, 2011*a*, 2012), only a few lack Kranz anatomy. These are the single-celled C_4 plants occurring in two terrestrial C_4 lineages of the Chenopodiaceae, a C_4 lineage of diatoms, and two lineages in the Hydrocharitaceae, a family of aquatic angiosperms (Bowes, 2011; Edwards and Voznesenskaya, 2011; Sage *et al.* 2011*a*). In terrestrial plants, variants of C_4-Kranz anatomy have independently evolved at least 60 times, making the Kranz syndrome one of the most convergent structural types in the living world (Sage *et al.* 2011*a*; Edwards and Voznesenskaya, 2011).

Kranz anatomy encompasses many distinct forms (Hattersley and Watson, 1992; Edwards and Voznesenskaya, 2011; Kadereit *et al.*, 2012; Freitag and Kadereit, 2013). The inner layer of K cells can be derived from parenchymatous bundle sheath (eudicots and many monocots), a mestome sheath around the vascular bundle (monocots only), or a sheath of parenchymatous cells around layers of water storage cells (eudicots only; Brown, 1975; Dengler and Nelson, 1999; Edwards and Voznesenskaya, 2011; see Supplementary Figs S1, S2 for examples). Kranz cells are generally more

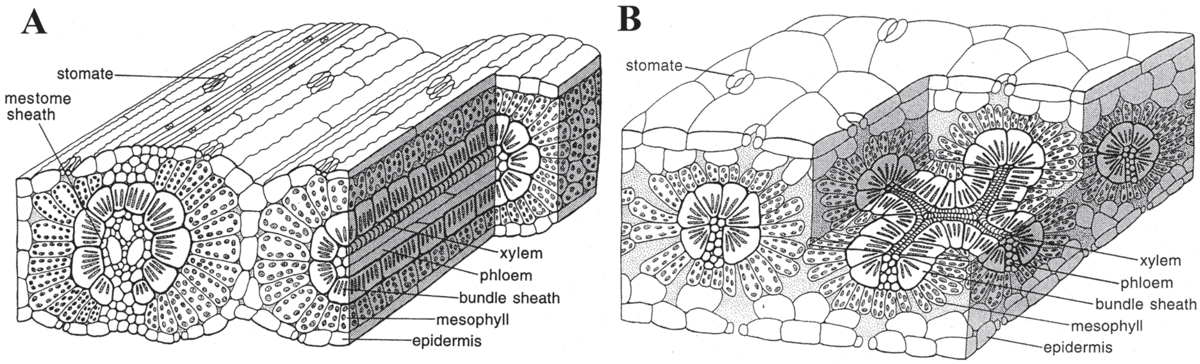

Fig. 1. Diagrams of classical forms of C_4 Kranz anatomy drawn from (A) an NAD-malic enzyme type of C_4 grass (*Panicum capillare*) and (B) the NAD-malic enzyme type of C_4 eudicot *Atriplex rosea*. Note the radial arrangement of a single layer of mesophyll cells around a layer of parenchymatous bundle sheath cells, and the presence of a mestome sheath in the larger veins of the C_4 grass in panel A. See Supplementary Fig. S1 for micrographs of numerous C_4 Kranz types, including *A. rosea*. Reprinted from Dengler NG, Nelson T. 1999. Leaf structure and development in C_4 plants. In: Sage R, Monson R, eds. C_4 plant biology. San Diego: Academic Press, 133–172. www.elsevier.com.

conspicuous than the homologous cells of their C_3 relatives, owing to the presence of larger and more numerous chloroplasts, thick outer walls, tight packing around the vascular bundles or water-storage cells, and limited exposure to intercellular air spaces (Fig. 1, Supplementary Figs S1, S2; Brown, 1977; Hattersley and Watson 1992; Dengler and Nelson, 1999; Pyankov *et al.*, 2000; Edwards and Voznsesenskaya, 2011). Additionally, K cells in C_4 plants are commonly larger than the homologous cells of their more distant C_3 relatives; however, size differences between K cells and the equivalent layer in closely related C_3 relatives are often lacking (Hattersley *et al.*, 1982; Muhaidat *et al.* 2007; 2011; Christin *et al.* 2013). Chlorenchymatous M cells between veins are reduced in number in C_4 relative to C_3 leaves, such that only one layer of photosynthetic M cells surrounds the K cells, and there is extensive wall-to-wall contact between the K and M cells (Fig. 1; Supplementary Figs S1, S2; Brown, 1977; Hattersley and Watson, 1992; Edwards and Voznesenskaya, 2011). This reduction in M cell layers minimizes the resistance to metabolite flux between the M and K cells (Bräutigam and Weber, 2011). In some Kranz types, an extra layer of cells lies between the M and K cells (Edwards and Voznesenskaya, 2011). The most common example of this occurs in grasses and sedges where an additional layer of cells with few chloroplasts separates M cells from mestome sheath cells where CO_2 is concentrated (Supplementary Fig. S2C; Hattersley and Watson, 1992; Soros and Dengler, 2001).

The many versions of the C_4 Kranz syndrome are also associated with distinct ultrastructural changes that are essential for C_4 function (Voznesenskaya and Gamaley, 1986; Hatch 1987; Hattersley and Watson, 1992; Dengler and Nelson, 1999; Edwards and Voznesenskaya, 2011). These include variation in organelle size, number, and position within the K cells (Dengler and Nelson, 1999; Voznesenskaya *et al.*, 1999, 2007, 2010; 2013; Koteyeva *et al.*, 2011; Muhaidat *et al.*, 2011; Sage *et al.*, 2011*b*; Bissinger *et al.*, 2014). Additionally, many C_4 monocots contain suberin in the wall of the K cells, a feature that is absent from the eudicots (Hattersley and Browning, 1981; Edwards and Vozensenskaya, 2011; Mertz and Brutnell, 2014). Suberin slows diffusive efflux, thus helping to trap CO_2 in the K cells (Laetsch, 1974; Mertz and Brutnell, 2014). Kranz cells with suberized walls often have centrifugally positioned organelles, whereas in leaves lacking suberized walls, the chloroplasts typically occur along the inner, centripetal region of the K cell (Supplementary Figs S1B–D; Hattersley and Watson 1992; Dengler and Nelson, 1999). The organelles of K cells are also altered to meet the different requirements of the three biochemical subtypes of C_4 photosynthesis. For example, photosystem II is depleted in the K cell chloroplasts of the NADP-ME subtypes, but not in the K-cell chloroplasts of the NAD-ME subtypes (Hattersley and Watson 1992; Dengler and Nelson, 1999; Edwards and Voznesenskaya, 2011; Furbank, 2011). In the NAD-ME subtype, the decarboxylating enzyme occurs in the mitochondria, whereas in the NADP-ME subtype, it is in the chloroplast (Hatch, 1987). As a result, K-cell mitochondria in NAD-ME species tend to be larger, more numerous, and closely associated with chloroplasts compared with NADP-ME species (Dengler and Nelson, 1999; Voznesenskaya *et al.*, 2010; Koteyava *et al.*, 2011; Khoshravesh *et al.*, 2012; Oakley *et al.*, 2014). In the M cells, C_4 plants produce about half the number of chloroplasts as their C_3 relatives, and the C_4 chloroplasts cover much less of the M cell periphery than in C_3 plants (Stata *et al.*, 2014). This reduction in chloroplast number enhances CO_2 access to the PEP carboxylation sites in the cytosol of the C_4 M cell. Also, the cell walls between M and K cells are enriched in plasmodesmata, which increases the rate of metabolite exchange between the two cell types (Hattersley 1984; Evert *et al.* 1977; Botha, 1992; Bräutigam and Weber, 2011). In summary, when all features associated with Kranz anatomy are considered, it is apparent that it represents a highly sophisticated suite of structural adaptations that not only establish the necessary compartmentalization required by the C_4 carbon concentrating mechanism (CCM), but also produces the subcellular intricacy needed for efficient C_4 photosynthesis.

How Kranz anatomy evolved remains one of the great mysteries of plant biology, and has recently become a hot topic because of ongoing efforts to engineer C_4 photosynthesis into C_3 crops, and the recognition that C_4 evolution is a major event in the formation of the modern biosphere (Edwards *et al.*, 2010; Covshoff and Hibberd, 2012; Christin *et al.*, 2013; Slewinski, 2013). Biologists are now in a much better position to resolve the Kranz enigma, as new developmental models and genomic tools facilitate the linkage of traits with the underlying genetic control (Covshoff *et al.*, 2012, 2014; Williams *et al.*, 2013; Fouracre *et al.*, 2014). Long-standing concepts of C_4 evolution can also be examined using phylogenetically informed comparisons that include C_3–C_4 intermediate species from multiple lineages (McKown and Dengler, 2007; Muhaidat *et al.*, 2011; Christin *et al.*, 2011, 2013; Khoshravesh *et al.*, 2012; Ocampo *et al.*, 2013; Sage *et al.*, 2013). Of particular value have been phylogenies with enough species coverage to identify close, sister taxa of C_3 and C_4 plants and numerous species with traits that are intermediate between the C_3 and C_4 conditions (McKown *et al.*, 2005; Sage *et al.*, 2007; Feodorova *et al.*, 2010; Christin *et al.*, 2011; Kadereit and Freitag, 2011; Roalson, 2011; Grass Phylogeny Working Group II, 2012; Khoshravesh *et al.*, 2012; Freitag and Kadereit, 2013; Ocampo *et al.*, 2013; Bissinger *et al.*, 2014). As a result, it has been possible to propose models of C_4 evolution that postulate, and then test, the importance of intermediate steps (Monson and Rawsthorne, 2000; Sage 2004; Sage *et al.*, 2012; Heckmann *et al.*, 2013; Williams *et al.*, 2013). A major aspect of these models has been the origin of Kranz anatomy.

In this review, we present a structure-function analysis addressing how Kranz anatomy may have evolved (see Fouracre *et al.*, 2014 for developmental perspectives of the issue). We begin by describing the conceptual models of C_4 evolution proposed by Monson and Rawsthorne (Monson *et al.*, 1984; Rawsthorne, 1992; Rawsthorne and Bauwe, 1998; Monson, 1999; Monson and Rawsthorne, 2000) as modified by Sage *et al.*, (Sage, 2001, 2004; Sage *et al.*, 2012). These models postulate a central role for glycine shuttling in the evolution of the C_4 pathway. We also discuss the importance of photorespiration and present a case that Kranz anatomy originated as a structure to enable the trapping and recycling of photorespired CO_2. Photorespiration has been termed the "bridge to C_4 photosynthesis" because in dealing with its consequences, many of the structural features essential to C_4 photosynthesis first evolved (Bauwe, 2011). As part of this discussion, we examine recent papers evaluating the critical initial phases of C_4 evolution that occur in the C3 relatives of C_4 clades (for example, Muhaidat *et al.*, 2011; Christin *et al.*, 2013; Sage *et al.*, 2013; Williams *et al.*, 2013). These close C_3 sisters exhibit changes in organelle size, number and location that are associated with changes in the size and shape of the bundle sheath cells, such that an incipient version of Kranz anatomy is apparent. The term "proto-Kranz" has been coined to describe this condition, which may represent the initial phase of C_4 evolution (Muhaidat *et al.*, 2011; Sage *et al.*, 2012; 2013).

Before proceeding, we define and justify our use of certain key terms to avoid confusion with earlier uses and to have a system that allows us to delineate evolutionary transitions in anatomical forms and photosynthetic physiologies. The term C_2 photosynthesis refers to a CCM that uses a photorespiratory glycine shuttle to concentrate CO_2 into an inner, BS-like compartment from the M tissue. This physiology has commonly been called C_3–C_4 intermediacy, but "C_3–C_4 intermediate" is inappropriate as it equates one specific trait with an evolutionary process that is comprised of many transitional characteristics, not just the glycine shuttle. In addition, the glycine shuttle is found in many species having no relationship to C_4 clades, and thus are not technically C_3–C_4 intermediates (Sage *et al.*, 2011*a*). Furthermore, "C_2" refers to the number of carbon atoms in the glycine molecule that transports CO_2 into the inner compartment, in the same manner that "C_4" refers to the four-carbon compound that transports CO_2 into the K cells. With respect to anatomical terminology, we restrict our definition of Kranz anatomy to those anatomical features where a wreath-like arrangement of M and BS-like cells enables a functioning CCM. This follows Haberlandt's (1914) suggestion that the Kranz-type has a distinct functional adaptation. By this definition, C_3 taxa with enlarged BS cells that have been listed as having Kranz anatomy (see for example, Metcalfe and Chalk, 1979, pages 214–215) would not have it, whereas the anatomical specializations associated with the C_4 and C_2 CCMs would represent two versions of Kranz anatomy. For clarity, we refer to the pronounced wreath-like anatomy of C_4 species as "C_4-Kranz", and the simplified wreath-like anatomy of C_2 species as "C_2-Kranz" (see Supplementary Fig. S2 for examples of each). "Sub-Kranz" might be a logical alternative to C_2-Kranz, but we feel this is inadequate as it implies the anatomy of C_2 species is an incomplete version of C_4-Kranz, rather than a structural adaptation in its own right that enables efficient function of the C_2 CCM. Sub-Kranz also does not connect the anatomy to the specific physiological adaptation, and can be confused with proto-Kranz, the term we use for anatomical changes in C_3 species that precede C_2-Kranz. Finally, we use the term BS (bundle sheath) cells in place of K cells because we repeatedly refer to the evolutionary transition from BS-like cells lacking a CCM to Kranz cells with a CCM, and the distinction between the two may not always be clear.

The Monson family of models for C_4 evolution

The high number of C_4 origins allow for the testing of evolutionary hypotheses using the methods of comparative biology, where each lineage represents an independent observation of one evolutionary transition (Ackerly, 1999; Christin *et al.*, 2013). Using such approaches, the evidence from the many C_4 lineages consistently supports gradual models of C_4 origin, with a critical intermediate role for a glycine shuttle that concentrates photorespired CO_2 into a BS-like compartment (Fig. 2; Monson and Rawsthorne, 2000; Sage *et al.*, 2012; Williams *et al.*, 2013). The glycine shuttle CCM was first proposed by Monson *et al.* (1984) to explain the photosynthetic physiology of the C_3–C_4 intermediate species known at that time (Rawsthorne *et al.*, 1988, Rawsthorne, 1992 and Monson 1999 for follow-ups). Glycine shuttling has since been identified in over 50 C_2 species from 20 or so evolutionary lineages

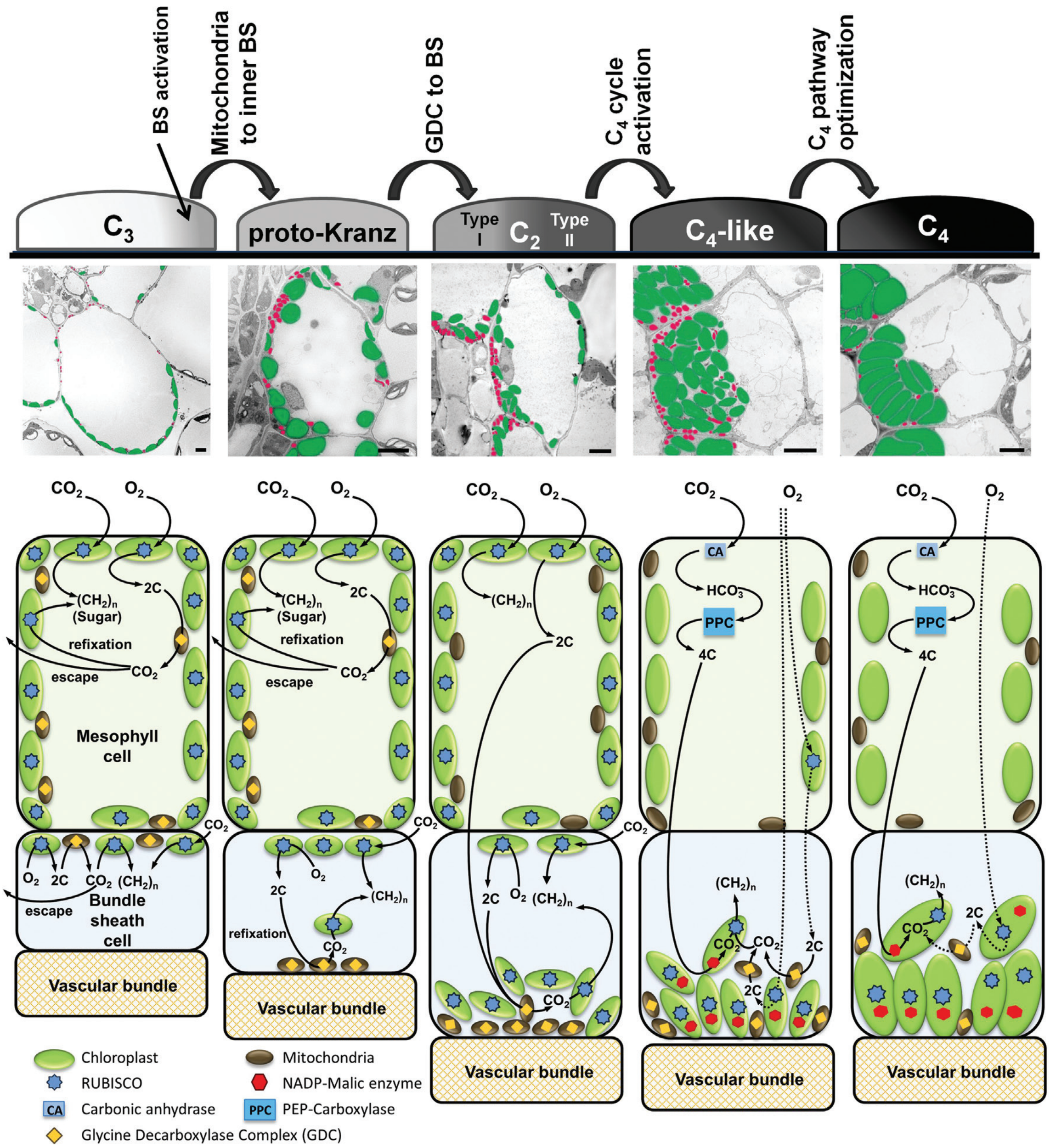

Fig. 2. A diagram illustrating the evolutionary progression from C_3 to C_4 photosynthesis via three distinct phases termed proto-Kranz, C_2 photosynthesis (C_2), and C_4-like photosynthesis. Arrows indicate the major changes between the phases. Note that bundle-sheath (BS) activation occurs within the C_3 group as indicated by the transition to grey shading; this refers to the increase in photosynthetic activity in the BS following an increase in organelle numbers and BS cell size. Immediately below are false-colour transmission electron micrographs showing chloroplasts (green) and mitochondria (red) for five *Flaveria* species that are classified as C_3, proto-Kranz, C_2, C_4-like, and C_4 plants. The bottom row illustrates carbon flow in the mesophyll (M) and BS tissues of the C_3 and proto-Kranz types, and between the M and BS in the C_2, C_4-like, and C_4 types. 2C indicates the two-carbon photorespiratory metabolite glycine; $(CH2)_n$ refers to leaf carbohydrate. Type I refers to C_2 photosynthesis and little associated C_4 cycle; Type II refers to C_2 photosynthesis with a modest C_4 cycle. Developed from Edwards and Ku, 1987; Moore *et al.*, 1987*b*; Ku *et al.*, 1991; Monson and Rawsthorne, 2000; Muhaidat *et al.*, 2011; and Sage *et al.*, 2012. Bars=5 μm. Explanation: *Flaveria cronquistii*, *F. robusta*, and *F. linearis* demonstrate the development of BS from an expanded, activated C3 condition to the mitochondria-enriched BS of the proto-Kranz and C_2 conditions. The main difference between these proto-Kranz and C_2 species is the high expression of glycine decarboxylase (GDC) in the M cells of *F. robusta*, compared with low expression of GDC in the M cells of *F. linearis* (not shown). The shift from the C_2-Kranz to C_4-Kranz forms is accompanied by an enlargement of BS chloroplasts and a reduction in BS mitochondria in this C_4 NADP-ME lineage. With respect to carbon flow, the M and BS cells in C_3 plants operate independently, with each assimilating O_2 and CO_2 and processing the fixation products to either CO_2 (via glycine decarboxylase, GDC, in the mitochondria) or carbohydrate (via photosynthesis). The CO_2 produced by GDC can then either escape the cell or be refixed. In proto-Kranz species, the movement of mitochondria and a few chloroplasts to the inner wall of the BS cells forces the glycine formed by outer chloroplasts to migrate to the inner BS for decarboxylation, with the released CO_2 accumulating and increasing Rubisco efficiency. This represents a single-celled, BS-specific glycine shuttle. In Type I C_2 species, GDC is largely restricted to BS cells, so that photorespiratory glycine diffuses to GDC located in centripetal mitochondria. The released CO2 accumulates and enhances Rubisco activity in the numerous chloroplasts in the inner BS. This is the two-celled photorespiratory glycine shuttle that boosts BS CO_2 levels. In the C_4-like pattern, a strong C_4 biochemical cycle moves 4C organic acids into the BS, whereas a weak two-celled glycine shuttle remains to process any glycine produced by the residual Rubisco in the M cells. In most C_4 leaves, the only way to move carbon from the M to BS cells is via the C_4 metabolic cycle involving PEP carboxylation.

Table 1. *The classification of the known C_3–C_4 intermediate species into proto-Kranz, C_2 photosynthesis, and C_4-like photosynthesis*

A clade of closely related C_4 species is also listed, if relevant. A listing of C_2 alone indicates the strength of C_4 metabolism is unknown. Compiled from Table 2 of Sage *et al.*, 2011a; Table V in Sage *et al.*, 1999 and references listed.

C_2 clade	Species	Photosynthetic category	Closely related C_4 clade	Reference
Amaranthaceae	*Alternanthera ficoides*	Type I C_2	*Alternanthera*	Rajendrudu *et al.*, 1986
	A. tenella	Type I C_2	*Alternanthera*	as with *A. ficoides*
Asteraceae	*Flaveria pringlei*	Proto-Kranz	*Flaveria* A, B	Edwards & Ku, 1987; Ku *et al.* 1991; McKown *et al.*, 2005; Vogan and Sage, 2011; Sage *et al.*, 2013
	F. robusta	Proto-Kranz	*Flaveria* A, B	as with *F. pringlei*
	F. sonorensis	Type I C_2	*Flaveria* A, B	as with *F. pringlei*
	F. ramosissima	Type II C_2	*Flaveria* A	as with *F. pringlei*
	F. palmeri	C_4-like	*Flaveria* A	as with *F. pringlei*
	F. vaginata	C_4-like	*Flaveria* A	as with *F. pringlei*
	F. angustifolia	Type I C_2	*Flaveria* B	as with *F. pringlei*
	F. anomala	Type II C_2	*Flaveria* B	Edwards and Ku, 1987; Ku *et al.*, 1991
	F. chloraefolia	Type I C_2	*Flaveria* B	as with *F. pringlei*
	F. pubescens	Type II C_2	*Flaveria* B	Edwards and Ku, 1987; Ku *et al.*, 1991
	F. linearis	Type II C_2	*Flaveria* B	as with *F. pringlei*
	F. floridana	Type II C_2	*Flaveria* B	as with *F. pringlei*
	F. oppositifolia	C_2	*Flaveria* B	as with *F. pringlei*
	F. brownii	C_4-like	*Flaveria* B	as with *F. pringlei*
Parthenium	*P. hysterophorus*	Type I C_2	None	Edwards and Ku, 1987; Moore *et al.*, 1987*a*
Boraginaceae	*Heliotropium karwinskyi*	Proto-Kranz	Mexican C_4 clade	Frohlich, 1978; Vogan *et al.*, 2007; Muhaidat *et al.*, 2011
	H. procumbens	Proto-Kranz	None	as with *H. karwinskyi*
	H. convolvulaceum	Type I C_2	Mexican C_4 clade	as with *H. karwinskyi*
	H. racemosum	Type I C_2	Mexican C_4 clade	as with *H. karwinskyi*
	H. greggii	Type I C_2	S. American C_4 clade	as with *H. karwinskyi*
	H. lagoense	C_2	S. American C_4 clade	as with *H. karwinskyi*
Brassicaceae	*Diplotaxis tenuifolia*	Type I C_2	None	Apel *et al.*, 1997
	Diplotaxis erucoides	C_2	None	Apel *et al.*, 1997
	Diplotaxis muralis	C_2	None	Apel *et al.*, 1997
	Moricandia arvensis	Type I C_2	None	Holaday and Chollet, 1984
	M. nitens	C_2	None	as with *M. arvensis*
	M. sinaica	C_2	None	as with *M. arvensis*
	M. spinosa	C_2	None	as with *M. arvensis*
	M. suffruticosa	C_2	None	as with *M. arvensis*
Chenopodiaceae	*Sedobassia sedoides*	C_2	Camphorosmae	Freitag and Kadereit, 2013; this study
	Salsola montana	Proto-Kranz	None	Voznesenskaya *et al.*, 2013
	S. arbusculiformis	Type I C_2	None	Voznesenskaya *et al.*, 2001, 2013
	S. divaricata	Type I C_2	None	Voznesenskaya *et al.*, 2013
Cleomaceae	*Cleome paradoxa*	Type I C_2	*Cleome angustifolia*	Voznesenskaya *et al.*, 2007; Feodorova *et al.*, 2010
Euphorbiaceae	*Euphorbia acuta*	Type I C_2	*Euphorbia* subgenus *Chamaesyce*	Sage *et al.* 2011*b*; Yang and Berry, 2011
	E. johnstonii	C_2	*Euphorbia* subgenus *Chamaesyce*	as with *E. acuta*
Molluginaceae	*Mollugo nudicaulis*	Type I C_2	*Mollugo cerviana*	Christin *et al.*, 2011
	M. verticillata	Type II C_2	*Mollugo cerviana*	Edwards and Ku, 1987; Christin *et al.*, 2011
Nyctaginaceae	*Bouganvillea cv.* Mary Palmer	C_2	None	Sabale and Bhosale, 1984
Portulacaeae	*Portulaca cryptopetala*	Type I C_2	*Portulaca*	Voznesenskaya *et al.*, 2010; Ocampo *et al.*, 2013
Scrophulariaceae	*Anticharis spp.*	Multiple C_2 candidates from herbarium specimens	*Anticharis*	Khoshravesh *et al.*, 2012
Cyperaceae	*Eleocharis spp*	Muliple C2 candidates	Unknown	Roalson *et al.*, 2010
Hydrocharitaceae	*Vallisneria spralis*	Uncertain	Unknown	Keeley, 1990

Table 1. *Continued*

C_2 clade	Species	Photosynthetic category	Closely related C_4 clade	Reference
Poaceae	*Homolepis aturensis*	C_2 anatomy	*Mesosetum* and/or *Arthropogon*	Grass Phylogeny Working Group II, 2012; Christin *et al.*, 2013
	Neurachne minor	Type I C_2	*Paraneurachne*	Hattersley *et al.*, 1986; Moore *et al.*, 1989; Christin *et al.*, 2012
	Panicum hylaeicum	Proto-Kranz	None	Holaday and Black, 1981; Brown *et al.*, 1983; Aliscioni *et al.*, 2003
	Steinchisma laxa	Proto-Kranz	None	as with *P. hylaeicum*
	S. cuprea	C_2	None	as with *P. hylaeicum*
	S. decipiens	C_2	None	as with *P. hylaeicum*
	S. exiguiflora	C_2	None	as with *P. hylaeicum*
	S. hians	Type I C_2	None	Edwards and Ku, 1987
	S. spathellosa	C_2	None	as with *P. hylaeicum*
	S. stenophylla	C_2	None	as with *P. hylaeicum*

(Table 1). Monson, Rawsthorne, and co-workers originally proposed a series of conceptual models for the evolutionary progression from C_3 to C_4 species, based on the variation observed in C_2 species of *Alternanthera, Flaveria, Mollugo, Moricandia, Neurachne*, and *Panicum*/*Steinchisma* (Monson and Moore, 1989; Monson, 1989, 1999; Rawsthorne, 1992; Rawsthorne and Bauwe, 1998; Monson and Rawsthorne, 2000). In recent years, numerous groups have built upon these conceptual models as data has become available from newly described C_3 to C_4 lineages (Sage, 2004; McKown and Dengler, 2007; Bauwe, 2011; Sage *et al.*, 2012). All of these models propose the glycine shuttle-type CCM as the key intermediate step between the C_3 and C_4 conditions. For this reason, we classify these as the Monson family of C_4 evolutionary models.

Figure 2 presents a schematic of C_4 evolution that follows from Monson and Rawsthorne (2000) and a recent iteration in Sage *et al.* (2012). For simplicity, we present the model as a flow scheme that documents the transition from C_3 to C_4 as moving through a series of intermediate phases; these correspond to known physiological states in existing lineages, and their order is consistent with phylogenetic patterns observed in those lineages. Three distinct intermediate phases are delineated, which we term (i) proto-Kranz, (ii) C_2 photosynthesis or the photorespiratory glycine shuttle, and (iii) C_4-like photosynthesis (Fig. 2). Four key transitions are noted. The first is BS activation, which occurs within the C_3 condition. Activation of the BS occurs when the BS cells engage in substantial photosynthetic activity owing to increases in their size and chloroplast number (Gowik and Westhoff, 2011; Sage *et al.*, 2013). *Flaveria cronquistii* is representative of a C_3 plant with an activated BS (Fig. 2). The key transitions following BS activation are the shift in the location of mitochondria from the outer to the inner BS, the localization of glycine decarboxylase (GDC) to the BS cells, and the activation of the C_4 metabolic pump (Fig. 2). Figure 2 also indicates the transition from a Type I to Type II condition within the C_2 phase. In the Type I subphase, the glycine shuttle alone concentrates CO_2 in the BS, whereas in the Type II subphase, the glycine shuttle is accompanied by modest C_4 metabolism. This follows the delineation of Type I and II C_3–C_4 intermediates by Edwards and Ku (1987).

The scheme in Figure 2 is conceptual and qualitative in nature. In the past year, two independent efforts have developed more complex, quantifiable models that use an adaptive landscape approach to analyse the details of the C_4 evolutionary process (Heckmann *et al.* 2013; Williams *et al.*, 2013). Heckmann *et al.* (2013) use a theoretical photosynthesis model (von Caemmerer, 2000) to quantify a fitness landscape across which evolutionary trajectories are modelled for the following six parameters: (i) fraction of Rubisco in the M tissue, (ii) Rubisco turnover capacity, (iii) fraction of GDC activity in the BS, (iv) C_4 cycle activity, (v) the K_m of PEP carboxylase for bicarbonate, and (vi) the conductance of the BS for gases (Heckmann *et al.*, 2013) In the model, these six traits were randomly altered between C_3 and C_4 values. If fitness increased following the single trait change, the trait could be fixed, and then built upon if a subsequent trait change increased fitness. This iterative process continued until the modelled phenotypes arrived at the C_4 condition for all traits. With respect to Kranz evolution, Heckmann *et al.* (2013) present two important findings. First, the formation of a glycine shuttle (and the C_2-Kranz anatomy that enables glycine shuttling) is the critical early phase in the biochemical evolution of C_4 photosynthesis. This theoretical result independently supports the empirical findings summarized in Fig. 2. Second, an extensive series of changes representing the biochemical evolution of the C_4 pathway largely corresponds to the "C_4 cycle activation" and "optimization" steps in Fig. 2 and thus would also correspond to the transition from C_2-Kranz to C_4-Kranz. Heckmann *et al.* (2013) did not directly model any specific anatomical change, but did include a number of parameters whose trait values would encompass anatomical changes. Of these, reduction in the BS conductance to CO_2 efflux is modelled to occur late, after activation of the C_4 biochemical cycle. Reduced BS conductance would largely reflect structural evolution, for example through thickening of the outer BS wall (von Caemmerer and Furbank, 2003).

In Williams *et al.* (2013), a meta-analysis of 43 studies of C_3–C_4 intermediates was used to quantify 16 biochemical, anatomical, and cellular traits to parameterize a phenotypic landscape. The evolution of C_4 photosynthesis across this landscape was then modelled as a transition network, and a time-ordered acquisition of traits was predicted based on the series of networks that were most compatible with the meta-analysis. For eudicots, the trait appearance predicted by the model was consistent with the qualitative scheme depicted in Fig. 2, in that changes in vein density, BS cell size, and GDC specificity occur early in C_4 evolution to establish the proto-Kranz and C_2-like conditions. Most of the biochemical changes were modelled to occur later, in what would correspond to the C_4 cycle activation and optimization phases of Fig. 2. The order of trait appearance in monocots differed, but Williams *et al.* (2013) had a limited set of C_3–C_4 intermediate grasses to parameterize the model, and so these predictions are tentative.

At this point, we evaluate the empirical and theoretical evidence for the structural changes that are thought to have occurred during C_4 evolution. We begin by discussing the anatomical traits in C_3 plants that may have enabled the initiation of C_4 evolution.

Setting the stage—the rise of anatomical enablers in the C_3 flora

Although C_4 photosynthesis evolved in taxonomic groups scattered throughout the angiosperm phylogeny, it tends to cluster in three major clades: the grasses (22–24 independent origins; GWPGII, 2012), the Caryophyllales (23 independent origins; Sage *et al.*, 2011*a*), and the sedges (six independent origins; Besnard *et al.*, 2009). As striking as this clustering is, the complete absence of C_4 photosynthesis in diverse and adaptable lineages such as the large orders containing the legumes, roses, lilies, and orchids is also noteworthy. Many of these groups are common in the same habits as C_4 species and numerous genera within these orders have evolved CAM, indicating photosynthetic flexibility (Smith and Winter, 1996; Sage, 2002). These patterns suggest there may be a series of predisposing traits that facilitate C_4 evolution in some taxa, whereas the lack of such traits may preclude C_4 evolution in other taxa. Preconditioning traits in C_3 species that may promote diversification of Kranz tissues include high vein density and enlarged BS cells (Sage, 2004; Muhaidat *et al.*, 2011; Sage *et al.*, 2012; Christin *et al.*, 2013; Griffiths *et al.*, 2013).

The identification of most lineages of C_4 photosynthesis has allowed for an evaluation of the environmental conditions where the C_4 pathway arose. In the eudicots, centres of origin have been postulated for 35 of the 36 known clades and it is possible to identify centres of origin for a handful of grass lineages (Sage *et al.*, 2011*a*; Christin *et al.*, 2012). The centres of origin generally correspond to hot, monsoon-affected regions, or non-monsoon areas where there is sufficient soil moisture to support summer photosynthesis. Most areas also correspond to where periodic aridity and low atmospheric humidity promote recurring episodes of water and/or salinity stress. Salinity seems to be a particularly important driver for C_4 evolution in the Chenopodiaceae lines of central Asia (Djamali *et al.*, 2012; Kadereit *et al.*, 2012; Sage *et al.*, 2011*a*). These conditions maximize the potential for photorespiration, but also create high evapotranspiration potentials that could lead to hydraulic crisis in leaves should the stomata remain open, or restrict carbon gain should stomata close to conserve water (Osborne and Sack, 2012; Sage, 2013). The key role of the monsoons is that they supply moisture during the summer season, creating moist growing conditions in what is often a hot, low humidity setting (Sage *et al.*, 2012). In these conditions, high vein density in leaves is proposed to be adaptive because it can deliver water fast enough to maintain tissue water status and prevent premature stomatal closure (Sage, 2001, 2004; Osborne and Sack, 2012). Consistently, C_3 species from hot, semi-arid regions often have greater vein density (Roth-Nebelsick *et al.*, 2001). High vein density seems to be particularly common in the C_3 sister clades of many C_4 lineages (Osborne and Sack, 2012; Sage *et al.*, 2012; Griffiths *et al.*, 2013). For example, vein density approaches or equals C_4 values in C_3 sister groups of *Anticharis* (Khoshravesh *et al.*, 2012), *Cleome* (Marshall *et al.*, 2007; Voznesenskaya *et al.*, 2007), *Heliotropium* (Muhaidat *et al.*, 2011), *Euphorbia* (Sage *et al.*, 2011*b*), *Mollugo* (Christin *et al.*, 2011), and *Salsola* (Voznesenskaya *et al.*, 2013). In a survey of species from 54 related C_3 and C_4 species from 13 eudicot families, no statistical difference was observed in vein density between the means of the C_3 and C_4 groups (Muhaidat *et al.*, 2007). Many C_3 grasses that are sister to the C_4 grass clades also have reduced interveinal distance, reflecting elevated vein density (Christin *et al.*, 2013).

Large BS size is also considered an important anatomical feature that may be more common in dry environments. Larger BS cells are posited to improve hydraulic capacitance in leaves and thus buffer surges in transpiration caused by wind gusts (Sage, 2004; Griffiths *et al.*, 2013). As with increased vein density, increased BS size is commonly found in the C_3 relatives of C_4 clades. Most of the C_3 sister groups of C_4 lineages in the PACMAD clade of grasses have increased BS volumes relative to M volumes (Brown *et al.*, 1983; Christin *et al.*, 2012, 2013; Griffiths *et al.*, 2013). In *Flaveria* and related genera, enlarged BS cells are present in the C_3 species *F. cronquistii* (Fig. 2) and its sister genus *Sartwellia* (McKown and Dengler, 2007; Sage *et al.*, 2013). Large BS cells are also present in a C_3 *Euphorbia* that is sister to the C_2 clade in *Euphorbia* section *acutae* (Sage *et al.*, 2011*b*). In *Heliotropium*, the closest C_3 relatives to the C_4 clades have enlarged BS cells relative to less-related C_3 species (Muhaidat *et al.*, 2011). In *Atriplex,* the C_3 and C_4 species that are related enough to form fertile hybrids also have similar BS cell size (Oakley *et al.*, 2014). In the Muhaidat *et al.* (2007) comparison of 54 C_3 and C_4 species from 13 dicot families, C_3 species had on average smaller BS cells; however, the BS cell size of many C_3 taxa overlapped with that of their C_4 relatives.

Understanding how increased vein density and BS size facilitates Kranz evolution requires close examination of BS ultrastructure and morphology. In C_3 species that branch in sister positions to C_2 or C_4 species in the *Anticharis*, *Cleome*, *Euphorbia, Flaveria*, and *Heliotropium* phylogenies, enlarged BS cells protrude into the mesophyll, forming spongy-parenchyma-like cells (Fig. 2; Marshall *et al.*, 2007 for *Cleome*; Muhaidat *et al.*, 2011 for *Heliotropium*; Sage *et al.*, 2011*b* for *Euphorbia*; Sage *et al.*, 2013 for *Flaveria*). The BS cell protrusions enhance exposure to the intercellular air space (IAS), thereby allowing many chloroplasts to be positioned along the perimeter of the BS cell that faces the IAS, as shown for *F. cronquistii* (Fig. 2). Notably, as observed in C_3 species of *Euphorbia*, *Flaveria* and *Heliotropium*, the BS chloroplasts facing the IAS occur near mitochondria, in an identical arrangement as that in M cells (Muhaidat *et al.*, 2011; Sage *et al.*, 2011*b*; Sage *et al.*, 2013). This close arrangement of mitochondria and chloroplasts facilitates rapid flux of metabolites between the two organelles during photorespiratory metabolism (Busch *et al.*, 2013). Enhancement of chloroplast numbers against the IAS wall of the BS cells is strong evidence that the BS has become heavily engaged in photosynthetic carbon assimilation, or following the terminology of Gowik and Westhoff (2011), the BS has become "activated". Photosynthetic activation of the BS is suggested to compensate for the loss of M cell volume as veins become more abundant in the leaf and BS cells expand (Sage *et al.*, 2012; 2013). Its significance for C_4 evolution is that the BS cells begin to generate large amounts of photorespiratory CO_2 in hot climates of low atmospheric CO_2. This formation of photorespired CO_2 represents an opportunity for improved carbon gain if the CO_2 production can be localized to a BS region where it can be trapped and refixed. As discussed next, the evolution of CO_2 trapping and refixation is proposed to give rise to the proto-Kranz condition and the first definitive step in C_4 evolution.

The proto-Kranz condition

As first described for two *Heliotropium* species (*H. procumbens* and *H. karwinskyi),* the proto-Kranz condition consists of enlarged BS cells relative to a typical C_3 *Heliotropium* species, and the BS tissue is more circular in outline than in the uneven edge produced by enlarged, spongy-like BS cells of the sister C_3 species *H. tenellum* (Muhaidat *et al.*, 2011). The more uniform BS outline in the proto-Kranz species is associated with a reduction in the exposure of the BS cells to the IAS. Mitochondria in the BS are larger in the two proto-Kranz *Heliotropium* species, and in *H. procumbens*, there are double the number of mitochondria relative to the C_3 sister species. Of particular note is the localization of 82–97% of the mitochondria to the inner wall of the BS in *H. karwinskyi* and *H. procumbens*, respectively (Muhaidat *et al.*, 2011). In *H. tenellum,* by contrast, mitochondria are spread around the cell periphery. The localization of mitochondria to the centripetal pole of the BS cells produced a distinct band of immunolocalization stain for glycine decarboxylase (GDC) along the inner edge of the BS, in a pattern that is similar to, though less intense, than that of C_2 species (Fig. 3A–C). Unlike the C_2 species, GDC is still common in the M cells of proto-Kranz species.

Muhaidat *et al.* (2011) drew attention to proto-Kranz anatomy described by Brown *et al.*, (1983) in the *Steinchisma* clade of grasses. *Steinchisma laxa* (formerly *Panicum laxum*) is sister to a C_2 clade of *Steinchisma*, whereas *Panicum hylaecium* is close to the *Steinchisma* clade (Aliscioni *et al.*, 2003). Both species have C_3 gas exchange characteristics and BS cells that are of similar size as the C_2 species of *Steinchisma*; however, the BS cells exhibit over 3-fold more BS chloroplasts, and *S. laxa* has 8-fold more mitochondria than a typical C_3 *Panicum* species (Morgan and Brown, 1980; Brown *et al.*, 1983). Nearly all of the BS mitochondria in *S. laxa* are arrayed along the inner BS wall where it contacts the vascular tissue. In *S. laxa*, there is also a layer of chloroplasts adjacent to the layer of mitochondria as is widely observed in C_2 species (Brown *et al.*, 1983). Curiously, in both *S. laxa* and *P. hylaecium*, many of the chloroplasts encapsulate the mitochondria (Brown *et al.* 1983), a feature that has been linked to increased refixation of photorespired CO_2 (Busch *et al.*, 2013).

In addition to *Heliotropium* and *Panicum*/*Steinchisma*, the proto-Kranz condition has recently been recognized in *Salsola montana* of the Chenopodiaceae (Voznesenskaya *et al.*, 2013) and two C_3 *Flaveria* species in the sunflower family, *F. pringlei* and *F. robusta* (Sage *et al.*, 2013). In *S. montana*, the leaf has a "sympegmoid" anatomy formed by concentric layers of mesophyll cells surrounding a central core of succulent water storage tissue and veins (Voznesenskaya *et al.*, 2013). Bundle-sheath cells occur beside the veins at the edge of the water storage tissue. Mitochondria in *S. montana* are localized to the wall against the vascular tissue in these BS cells, leading to its designation as a proto-Kranz species (Voznesenskaya *et al.*, 2013).

In *Flaveria*, detailed examination of the species branching at the basal nodes of the phylogeny has identified two species previously categorized as C_3 (*F. pringlei* and *F. robusta*) as having proto-Kranz features similar to those observed in *Heliotropium* (Sage *et al.*, 2013). In the *Flaveria* phylogeny, *F. pringlei* and *F. robusta* branch at nodes between the C_3 *F. cronquistii* node and the nodes for the C_2 species *F. sonorensis* and *F. angustifolia* (McKown *et al.*, 2005). In the basal branching *F. cronquistii* and its sister species *Sartwellia flaveriinae,* BS cells are enlarged with elongated spongy-like protrusions, whereas in *F. pringlei* and *F. robusta,* the BS cells have coalesced into a more even edged-sheath with low exposure to the IAS (Sage *et al.*, 2013). Bundle-sheath cells in *F. pringlei* and *F. robusta* are enlarged compared with a typical C_3 species such as sunflower but are actually smaller than their immediate C_3 sister species that branch lower in the phylogeny (McKown and Dengler, 2007; Sage *et al.*, 2013). This is due to the loss of the lobing observed in the expansive BS cells of *F. cronquistii*. In *F. pringlei* and *F. robusta*, organelle numbers are enhanced, and 75% or more of the BS mitochondria are centripetally located, which approximates the mitochondria distribution in the BS of C_2 species (Fig. 2; Sage *et al.*, 2013). Both *F. pringlei* and *F. robusta* have a distinct band of GDC stain along the inner BS wall, yet both also express GDC in the M mitochondria (Fig. 3D–F). This GDC distribution is similar to what has been reported for the proto-Kranz species in the genus *Heliotropium* (Fig. 3; Muhaidat *et al.*, 2011). In *F. robusta*, numerous chloroplasts also occur beside the

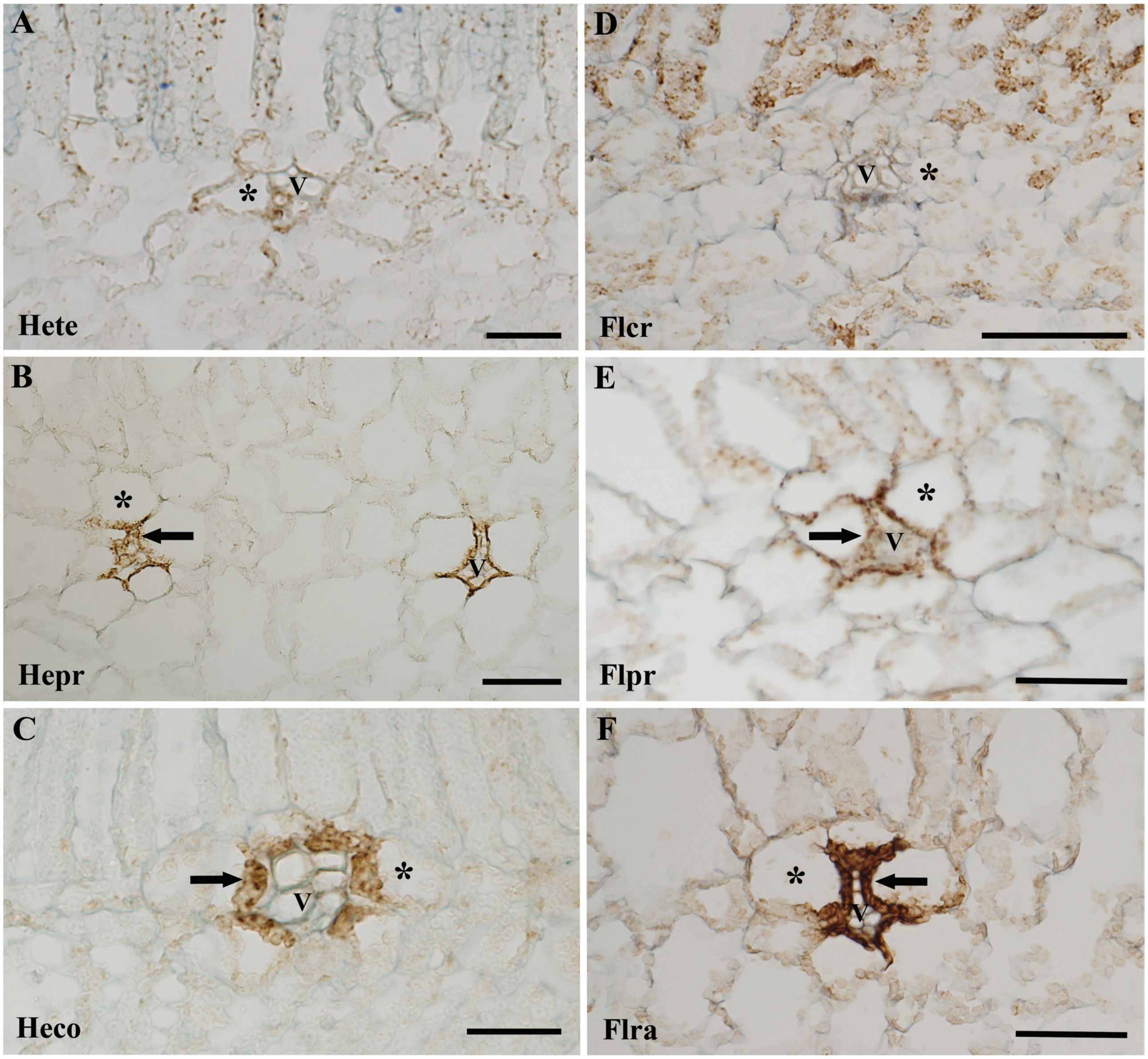

Fig. 3. *In situ* immunolocalization of GDC p-protein subunit in the leaves of C_3 (A, D), proto-Kranz (B, E), and C_2 (C, F) species in the genus *Heliotropium* (A–C) and *Flaveria* (D, E). Hete, *H. tenellum*; Hepr, *H. procumbens*; Heco, *H. convovulaceum*; Flcr, *F. cronquistii*; Flro, *F. robusta*; Flra, *F. ramosissima*. Brown stain indicates the presence of GDC. Asterisks indicate bundle sheath cells and arrows point out bundle sheath mitochondria. V indicates vascular tissue. Bars=50 μm.

centripetal BS mitochondria in a pattern similar to that of many C_2 species (Figs 2, 4; Sage *et al.*, 2013).

The observation that C_3 proto-Kranz species are closely related to C_2 species in four independent lineages supports a hypothesis that the proto-Kranz condition is an early phase of C_2 evolution, and in turn, C_4 evolution. If this is the case, it is logical to assume there is an adaptive benefit conferred by the proto-Kranz traits. Photosynthetic gas exchange responses demonstrate a subtle reduction of the CO_2 compensation point of photosynthesis (Γ), which could provide slight yet biologically meaningful enhancements in carbon gain at low intercellular CO_2 levels. In *S. laxa*, the gas exchange benefits are a 5–7 μmol CO_2 mol^{-1} air reduction in Γ across a range of O_2 levels, and increased sensitivity of Γ to variation in light intensity (Morgan and Brown, 1980; Sage *et al.*, 2013). In *H. procumbens* and *H. karwinskyi*, the benefit may be a slight reduction in the slope of the Γ versus O_2 response (Vogan *et al.*, 2007). In *Flaveria pringlei* and *F. robusta*, Γ is also reduced by 5–10 μmol mol^{-1} relative to the C_3 *F. cronquistii* and *Sartwellia flaveriae* (Sage *et al.*, 2013); however, no consistent gas exchange differences were observed in *Salsola montana* relative to its C_3 relatives (Voznesenskaya *et al.*, 2013). In *F. robusta*, Γ also exhibited greater light dependency than C_3 species (Sage *et al.*, 2013). Large reductions in Γ with an increase in light intensity indicate a C_2-type of CCM may be active in higher plants (Sage *et al.*, 2013). The greater light dependency in *F. robusta* was associated with a shift to lower intercellular CO_2 values (C_i) of the relationship between net CO_2 assimilation rate (A) and C_i, which is not observed in the C_3 species, but is pronounced

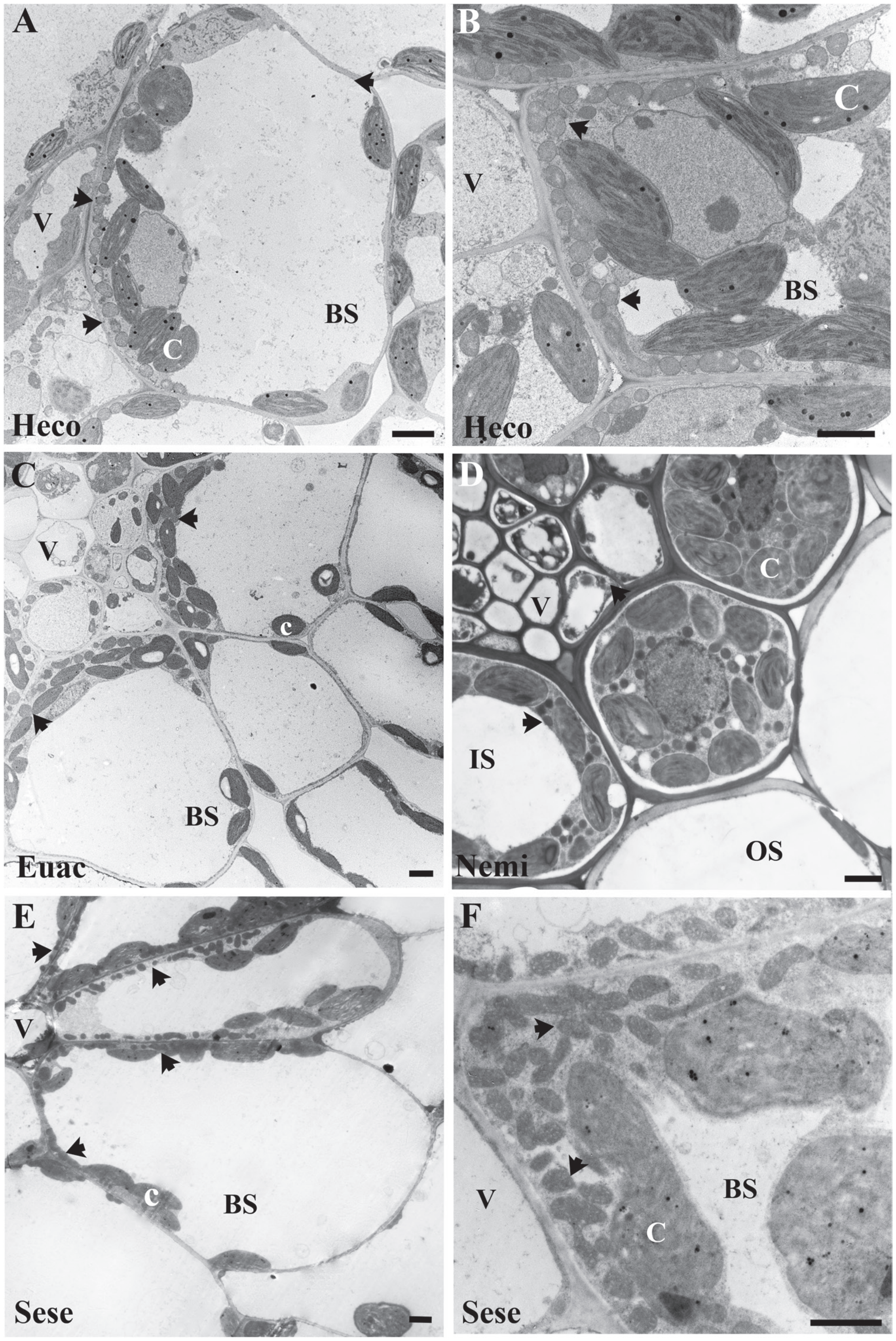

Fig. 4. The ultrastructure of bundle sheath cells in C_2 species of *Heliotropium convolvulaceum* (Boranginaceae) at (A) low magnification and (B) high magnification; (C) *Euphorbia acuta* (Euphorbiaceae); (D) *Nuerachne minor* (Poaceae); and *Sedobassia sedoides* (Chenopodiaceae) at (E) low magnification and (F) high magnification. Bars=2 μm.

in C_2 species. This was interpreted by Sage *et al.*, (2013) to indicate that *F. robusta* operates has a weak glycine shuttle which allows it to refix proportionally more photorespired CO_2 than C_3 species, although much less than in C_2 species. This refixation mechanism may represent the adaptive benefit of the proto-Kranz suite of traits.

The refixation mechanism for photorespiratory CO_2 in the proto-Kranz species may be nothing more than a single-cell glycine shuttle within the BS that arises when mitochondria become localized to the inner BS wall (Fig. 2). Numerous chloroplasts remain against the outer perimeter of the cell facing the IAS, and thus are presumably assimilating CO_2 and oxygenating RuBP. If the mitochondria have moved from a position near an outer chloroplast to the inner edge of the cell, any glycine formed during photorespiration would build up around the outer chloroplasts and diffuse to where GDC is localized, which in the proto-Kranz species would be in the rank of mitochondria along the centripetal wall of the BS cells (Sage *et al.*, 2013). The diffusion barrier presented by the tonoplast and vacuole would then restrict the efflux of the photorespired CO_2, causing it to accumulate and enhance photosynthesis within chloroplasts in the inner BS. It is also possible that the BS mitochondria receive glycine from the M tissue, which may happen in more than a trivial manner if photorespiration in the M cells exceeds the GDC capacity in the resident mitochondria. This could occur if the GDC capacity in M cells lags behind Rubisco oxygenase activity, which may happen in very hot climates during low CO_2 episodes, or if M GDC expression is reduced in proto-Kranz species. In either case, the increased number of BS mitochondria in proto-Kranz species indicates there is a rise in BS GDC capacity that might draw M glycine into the BS (Sage *et al.*, 2013). This would become an important source of CO_2 for the BS cells of the proto-Kranz species, and could establish conditions where additional reductions in M GDC allow for greater glycine flux to the BS, further enhancing carbon gain and thus facilitating positive selection for a stronger glycine shuttle (Sage *et al.*, 2012; Heckmann *et al.*, 2013).

The potential significance of the proto-Kranz traits is only recently recognized, and few species have been examined for this condition. It is possible that many species from hot climates have enlarged, activated bundle sheaths with a centripetal distribution of mitochondria. If this is the case, then there could be many possible candidates for evolving the two-tissue CCM of C_2 photosynthesis, and eventually, C_4 photosynthesis. Identification of additional proto-Kranz species will be essential for knowing whether the proto-Kranz condition is a common and perhaps essential early phase of C_4 evolution, and for studying the functional advantage of this trait.

Kranz anatomy in C_2 plants

In contrast to the diversity observed in C_4 Kranz anatomy, Kranz-like anatomy in C_2 species is fairly homogeneous, in part because the known C_2 taxa are largely from clades with a similar leaf anatomy (Supplementary Fig. S2). For example, all but three of the identified C_2 species occur in eudicot clades where C_4 relatives express the Atriplicoid-type of Kranz anatomy, which is the most common type in C_4 dicots (Sage *et al.*, 2011*a*). Also, the physiological options for C_2 photosynthesis are fairly uniform compared with the possibilities for the C_4 pathway. In Type-I C_2 photosynthesis, Rubisco is both the primary carboxylase (in M cells) and secondary carboxylase (in BS cells), there is one decarboxylase (GDC), and the energetics of the M and BS chloroplasts are similar (von Caemmerer, 1989; Monson and Rawsthorne, 2000). Thus, certain factors that lead to biochemical and ultrastructural diversification between C_4 lineages do not seem to be major issues in C_2 evolution. The structural variation in C_2 anatomy that is most evident occurs in the Australian grass *Neurachne minor*, the only C_2 species in the *Neurachne* clade where C_4 evolution occurs twice, and in C_2 species in the Chenopodiaceae that are related to C_4 species with the Salsoloid-type of Kranz anatomy (Hattersley *et al.*, 1986; Voznesenskaya *et al.*, 2001, 2013; Christin *et al.*, 2012). These variants are discussed below.

In most C_2 species, the distinguishing feature is a dense aggregation of chloroplasts and enlarged mitochondria along the inner periphery of the BS cells (Figs. 2, 4; Supplementary Fig. S2; Holaday *et al.*, 1984; Brown *et al.*, 1983; Moore *et al.*, 1987*a*; Hylton *et al.*, 1988; Brown and Hattersley, 1989; Monson and Rawsthorne, 2000; Christin *et al.*, 2011; Muhaidat *et al.*, 2011; Sage *et al.*, 2011*b*, 2012, 2013; Ueno *et al.* 2003; 2007; Voznesenskaya *et al.*, 2007, 2010, 2013). Glycine decarboxylase is abundant in these mitochondria, such that a dense band of immunolabel against GDC is observed along the inner BS of C_2 species in immunolocalization experiments (Fig. 3; Hylton *et al.*, 1988; Rawsthorne *et al.*, 1988; Ueno *et al.*, 2006; Voznesenskaya *et al.*, 2007; Muhaidat *et al.*, 2011; Sage *et al.*, 2011*b*, 2013). In the C_2 species with an inner rank of mitochondria, few if any mitochondria are present along the outer periphery of the cell (Muhaidat *et al.*, 2011; Sage *et al.*, 2011*b*, 2013; Voznesenskaya *et al.*, 2007, 2013). This polarity in mitochondrial placement is one of the distinguishing features in most of the C_2 species examined. The chloroplasts in the inner BS typically line up next to the rank of mitochondria (Figs 2, 4; Monson and Rawsthorne, 2000; Sage *et al.*, 2012; 2013). Rubisco and starch are abundant in these chloroplasts, and it is generally assumed they are photosynthetically engaged (Hylton *et al.*, 1988; Rawsthorne, 1992; Voznesenskaya *et al.*, 2001; Muhaidat *et al.*, 2011; Sage *et al.*, 2013). In many, but not all cases, the chloroplasts are abundant enough to form a near-continuous layer between the mitochondria and the vacuole (Holaday *et al.*, 1984; Brown and Hattersley, 1989; Muhaidat *et al.*, 2011; Sage *et al.*, 2013). This arrangement is particularly effective in enhancing the probability of photorespired CO_2 being captured and refixed by the inner chloroplasts before it can escape the cell (Rawsthorne, 1992). Many C_2 species also have chloroplasts along the outer BS periphery, but these are not associated with mitochondria as they are in C_3 species (Voznesenskaya *et al.*, 2007; 2010; 2013; Muhaidat *et al.*, 2011; Sage *et al.*, 2011*b*; Sage *et al.*, 2013). Hence, any photorespiratory metabolites produced by these chloroplasts will have to diffuse into the inner BS for metabolism.

Anatomically, the BS cells of C_2 species are generally more pronounced in leaf cross sections than they are in C_3 species, reflecting in most cases a larger BS cell size (Supplementary Fig. S2; McKown and Dengler 2007; Muhaidat *et al.*, 2011; Sage *et al.*, 2011*b*, 2013). With the pronounced clump of organelles lining the inner BS, the BS cells of C_2 species exhibit a modest wreath-like appearance that is apparent in cross sections and vein of leaf clearings, including leaves reconstituted from herbarium specimens (Supplementary Fig. S2; McKown and Dengler, 2007; Muhaidat *et al.*, 2011; Sage *et al.*, 2011b; Christin *et al.*, 2011; Khoshravesh *et al.*, 2012). This characteristic allows for relatively rapid screens for possible new C_2 species using herbarium material, which is important, as living C_2 plants are often unavailable. Carbon isotope screens do not generally identify C_2 species (Sage *et al.*, 2007). C_2 BS cells are rarely as distinctive as C_4 Kranz cells, which are more prominent owing to a larger and denser organelle mass (Figs 2, 4; supplementary Fig. S2).

In most C_2 species, the M tissue is reduced in prominence compared with C_3 relatives, as a result of larger BS cells and in many cases, greater vein density (Supplementary Fig. S2; Ueno *et al.* 2006; McKown and Dengler, 2007; Muhaidat *et al.*, 2011). However, unlike the case with C_4 Kranz, multiple layers of M cells remain around the BS cells and M:BS cell ratios rarely approach the low values observed in C_4 plants (McKown and Dengler, 2007, 2009; Voznesenskaya *et al.*, 2007, 2010; 2013). The ultrastructure of M cells of C_2 species changes little from their C_3 counterparts. C_2 and C_3 M cells of related plants have similar chloroplast numbers, distribution, and size (Stata *et al.*, 2014). GDC is often absent in the M cells, leading to the proposal that activation of the C_2 pathway follows a mutation that knocks out GDC expression in the M mitochondria (Monson and Rawsthorne 2000; Sage *et al.*, 2012). In *Cleome, Euphorbia*, *Heliotropium*, *Mollugo*, and *Portulaca*, there is no evidence for GDC expression in the M mitochondria of C_2 species (Marshall *et al.*, 2007; Muhaidat *et al.*, 2011; Sage *et al.*, 2011*b*; Voznesenskaya *et al.*, 2007, 2010). In *Flaveria*, however, the loss of GDC is gradual. C_2 *Flaveria* species branching lower in the phylogeny still express GDC protein and mRNA in the M mitochondria, whereas C_2 and C_4 *Flaveria* species branching in a more distal position have negligible GDC expression in M cells (Sage *et al.*, 2013; Schulze *et al.*, 2013).

The three exceptions to the typical C_2 Kranz anatomy described above are the grass *Neurachne minor*, two *Salsola* species of the Chenopodiaceae (*Sa. arbusculiformis* and *Sa. divaricata*) and the chenopod *Sedobassia sedoides*. In *N. minor*, the cells of an inner sheath that sit just inside a relatively empty outer sheath are co-opted to be the site of CO_2 concentration, and presumably, GDC localization (Fig. 4; Supplementary Fig. S2B; Hattersley *et al.*, 1986; Brown and Hattersley, 1989). In these cells, chloroplast and mitochondrial density are high, but there is no apparent pattern in their distribution (Fig. 4D). It is likely that the wall of the inner sheath, and the outer sheath layer of cells, provide a strong barrier to leakage of photorespired CO_2 such that the organelles need not be localized next to each other along the inner cell wall (Brown and Hattersley, 1989). In many succulent chenopods, the leaf anatomy is comprised of multiple layers of M cells around a central core of water storage cells (Voznesenskaya *et al.*, 2001, 2013). The inner M cell layer is co-opted as the site of CO_2 concentration in the C_2 chenopods and the C_4 species that have Salsaloid- and Kochioid-types of Kranz anatomy (Edwards and Voznesenskaya, 2011; Voznesenskaya *et al.*, 2001, 2013). In the C_2 species *Salsola arbusculiformis*, *Sa. divaricata*, and *Se. sedoides*, the inner Kranz-like layer where GDC is localized occurs adjacent to vascular cells along the periphery of the water storage cells, in what is interpreted to be an intermediate version of the Salsoloid Kranz anatomy (Voznesenskaya *et al.*, 2013; Freitag and Kadereit, 2013). In *Sa. arbusculiformis* and *Sa. divericata*, the BS mitochondria and chloroplasts are very abundant, occupying over a third of the cell-volume (Voznesenskaya *et al.*, 2001, 2013). In *Se. sedoides*, many mitochondria line the BS walls adjacent to vascular tissue and other BS cells, but avoid the outer BS facing the intercellular air space (Fig. 4E, F).

The transition from proto-Kranz to C_2-Kranz can be inferred in *Flaveria*, *Heliotropium* and *Steinchisma*, as indicated by the sister position of the proto-Kranz and C_2 species in their respective phylogenies. In *Salsola*, the proto-Kranz species *Sa*. *montana* is present on a close, yet separate branch of the phylogeny than the nearest known C_2 species (Voznesenskaya *et al.*, 2013). In *Flaveria* and *Heliotropium*, the changes are similar, being characterized by further enlargement of the BS tissue and increases in organelle size and number, resulting in more chloroplasts associating with the inner mitochondria (McKown and Dengler, 2007; Muhaidat *et al.*, 2011; Sage *et al.*, 2013). A reduction or loss of GDC expression is apparent in the M tissue, which when coupled with the larger and more numerous BS mitochondria, explains the reduction in the CO_2 compensation point to values that are half of the C_3 values (Muhaidat *et al.*, 2011; Sage *et al.*, 2013). In *Steinchisma*, the principal change between the proto-Kranz and C_2 species is an increase in chloroplast number and size in the inner BS region. Compared with the proto-Kranz *S. laxa*, the BS of the C_2 species *St. spathellosum* (formerly *Panicum schenckii*) has twice the number of mitochondria, 25% more chloroplasts, and three times as many peroxisomes; however, cell size does not differ (Brown *et al.*, 1983). In considering these examples, it is apparent that the formation of C_2 Kranz from the proto-Kranz condition requires multiple genetic changes and cannot be attributed to a single cause, such as GDC loss in the M tissue. GDC decline in M cells may be an important facilitator of the transition from proto-Kranz to C_2 Kranz, because it may establish a two-tissue glycine shuttle, with subsequent evolutionary selection creating the similar Kranz-like traits that occur repeatedly in the C_2 lineages (Sage *et al.*, 2012; Heckmann *et al.*, 2013; Schulze *et al.*, 2013). In any case, the multiple convergence on C_2 Kranz is strong evidence that this anatomy is specifically adapted for the C_2 pathway, in the same vein that C_4 Kranz is an adaptation for C_4 photosynthesis.

Within the C_2 condition, the major change is the shift from the Type I condition of C_2 photosynthesis only, to the Type II condition of C_2 photosynthesis and an accessory C_4 metabolic cycle (Edwards and Ku, 1987). In Type II species, the C_4 metabolic cycle can account for up to 50% percent of the initial carboxylation capacity, and reduce the CO_2 compensation point of photosynthesis to below 10 μmol mol^{-1} (Moore *et al.*, 1987*b*; Monson *et al.*, 1988; Monson and Rawsthorne, 2000). However, there are no major structural changes associated with the transition from the Type I to Type II modes, and the C_2 Kranz type are similar in Type I and Type II forms, as indicated by studies with *Flaveria* and *Mollugo* (Kennedy *et al.*, 1980; Holaday et al, 1984; Edwards and Ku, 1987; Monson and Rawsthorne, 2000).

Kranz anatomy in C_4-like plants

The C_4-like condition is only confirmed in three species, all of which occur in *Flaveria* (*F. brownii, F. palmerii*, and *F. vaginata*; Monson *et al.*, 1987; Moore *et al.*, 1989; Ku *et al.* 1991); however, isotopic and anatomical evidence from herbarium specimens indicate additional C_4–like species exist in *Blepharis*

(Acanthaceae; McDade, Sage, and Sage, unpublished) and *Anticharis* (Scrophulariaceae; Khoshravesh *et al.*, 2012). Although the diversity of known C_4-like species limits the ability to make broad inferences, the C_4-like species of *Flaveria* are well studied and thus, for *Flaveria* at least, provide a detailed observation of the late stages of C_4 evolution. *Flaveria palmerii* and *F. vaginata* are in clade A where they are sister to the full C_4 species of *Flaveria*; *F. brownii* occurs on a distinct phylogenetic branch, termed clade B and lacks immediate C_4 relatives (McKown *et al.*, 2005). On both clades A and B, Type II C_2 species branch just below the C_4 like species, indicating the C_4-like species arose from type II C_2 ancestors (McKown *et al.*, 2005).

The transition from Type II C_2 species to the C_4-like condition is marked by a dramatic rise in the activity of the C_4 cycle enzymes, increased water- and Rubisco-use efficiency of photosynthesis, and a large reduction in Rubisco and C_3 cycle activity in the M cells (Fig. 2; Moore *et al.*, 1987*b*; Ku *et al.*, 1991; Dai *et al.*, 1996; Monson and Rawsthorne, 2000; Kocacinar *et al.*, 2008; Vogan and Sage, 2011). PEPC and NADP-ME activities, for example, are 5-fold higher in the C_4-like species than the C_2 species and are similar to the C_4 values (Ku *et al.*, 1991). Also, in the C_4-like species, the percentage of ^{14}C label present in aspartate and malate exceeds 67%, compared with 46% in the highest Type II C_2 species (Moore *et al.*, 1987*b*) and CO_2 compensation points drop to within a few μmol mol^{-1} of C_4 values (Ku *et al.*, 1991; Dai *et al.*, 1996). These results demonstrate a strong enhancement of the C_4 metabolic cycle and corresponding reduction in the M C_3 cycle in what is considered to be the activation of the C_4 pathway (Sage *et al.*, 2012). C_4-like plants are not considered to be fully developed C_4 species because the localization of Rubisco into the BS is incomplete, the oxygen inhibition of photosynthesis is halfway between C_3 and C_4 values, and the carbon isotope ratios are below the C_4 range, although they are higher than in most C_3 species (Monson *et al.*, 1988; Ku *et al.*, 1991; Monson and Rawsthorne, 2000). In addition, PEPC, Rubisco and carbonic anhydrase may not have fully evolved the kinetic and regulatory properties of the isoforms in their close C_4 relatives (Engelmann *et al.*, 2003; Ludwig, 2011; Ludwig, 2013). The acquisition of these final set of characteristics that distinguish an efficient, fully expressed C_4 pathway occur in a final phase of C_4 evolution termed the optimization phase (Sage *et al.*, 2012).

Structurally, the Kranz anatomy of the C_4-like phase is best described in *F. brownii*. In *F. palmerii* and *F. vaginata*, the structural features are largely C_4 in nature and don't reveal much about the final phase before the acquisition of full C_4 Kranz anatomy (McKown and Dengler, 2007; Rahman, Sage, and Sage, unpublished). *Flaveria brownii* retains vestiges of the C_2 condition. The fraction of BS tissue in the leaf is also less in *F. brownii* than in C_4 leaves (Araus *et al.*, 1990). The bundle sheath ultrastructure of *F. brownii* is intermediate between Type II C_2 species and C_4 species: chloroplasts are larger and more numerous in *F. brownii* than in Type II species, but much shorter than in the C_4 *Flaveria* species such as *F. trinervia* (Fig. 2; Holaday *et al.*, 1984; Araus *et al.*, 1990). In *F. brownii*, many BS mitochondria occur along the interior of the centripetal wall of the BS cells, similar to the pattern observed in C_2 species, but markedly different than in *F. trinervia*, where mitochondria do not form distinct ranks along the inner BS periphery (Fig. 2; Holaday *et al.*, 1984; Brown and Hattersley, 1989; Araus *et al.*, 1990). As with the biochemical and physiological responses, it is safe to conclude that the Kranz anatomy of *F. brownii* is intermediate between the C_2 and C_4 Kranz modes.

Conclusion

Over the past 40 years, studies with species that exhibit intermediate traits support models that the evolution of C_4 photosynthesis is a staged affair, with the two-celled, photorespiratory glycine shuttle being a critical intermediate step. We propose here that there were four important events that facilitated the evolution of C_4 photosynthesis (Fig. 2). The first is the activation of the C_3 BS, such that in hot environments, high vein density and BS cells become photosynthetically engaged through greater exposure to intercellular air spaces and the acquisition of increased numbers of chloroplasts and mitochondria. These cells are completely C_3, but their enhanced physiological activity enables the formation of weak mechanisms to scavenge photorespiratory CO_2 via the second key event, the migration of mitochondria to the centripetal region of the BS cells. With the reorientation of some chloroplasts to the inner wall to join the mitochondria the proto-Kranz condition arises, and with it, the potential to establish facilitation cascades where the M GDC is reduced while BS GDC and organelle numbers sequentially increase, activating the C_2 photorespiratory CCM. This reduction in M GDC represents the third major event in C_4 evolution. In time, key components of the C_4 metabolic cycle are up-regulated to complement C_2 photosynthesis, and this is proposed to facilitate the next major event, the activation of the full C_4 pathway with the coincident decline of the C_3 pathway in M tissues. Once the C_4-like condition is achieved, evolutionary optimization adjusts many of the photosynthetic components to efficiently operate in the C_4 context, leading to fully developed C_4 photosynthesis. Many C_3–C_4 species from 20 or so lineages support various aspects of this model, although our understanding of the initial and end phases are heavily dependent upon just a few species from a couple of lineages. These handful of species may skew our impression of early and late events, and thus it is important to use phylogenetic analyses to identify and collect addition proto-Kranz and C_4-like species. By doing so, the amount of information available to parameterize models that can analyse and predict trajectories of C_4 evolution will substantially increase.

Supplementary data

Supplementary data are available at *JXB* online

Figure S1. Transverse sections showing the leaf anatomy of three C_4 species and a C_3 species from the PACMAD clade of grasses, and C_3 and C_4 species from three C_4 lineages of the Chenopodiaceae.

Figure S2. Transverse sections illustrating leaf anatomy of closely related C_3, C_2, and C_4 species from six lineages of C_4 photosynthesis. and a Canadian International Development Agency (CIDA) GCIAR-Canada linkage fund grant to TLS and RFS.

Acknowledgements

The authors thank Kate Sault, Matt Stata, Stefanie Sultmanis, and Troy Rennie for technical assistance. This research was supported by grants from the Natural Science and Engineering Research Council of Canada (grant nos. 155258-2008 to TLS and 154273-2012 to RFS) and a Canadian International Development Agency (CIDA) GCIAR-Canada linkage fund grant to TLS and RFS.

References

Ackerly DD. 1999. Comparative plant ecology and the role of phylogenetic information. In: Press MC, Scholes JD, Barker MG, eds. *Physiological plant ecology*. Oxford: Blackwell Science, 391–413.

Aliscioni SS, Giussani LM, Zuloaga FO, Kellogg EA. 2003. A molecular phylogeny of *Panicum* (Poaceae: Paniceae): tests of monophyly and phylogenetic placement within the Panicoideae. *American Journal of Botany* **90,** 796–821.

Apel P, Horstmann C, Pfeffer M. 1997. The *Moricandia* syndrome in species of the Brassicaceae - evolutionary aspects. *Photosynthetica* **33,** 205–215.

Araus JL, Brown RH, Bouton J, Serret MD. 1990. Inheritance of leaf anatomical characteristics in C_4 *Flaveria* plants. *Photosynthesis Research* **26,** 49–57.

Bauwe H. 2011. Photorespiration: the bridge to C_4 photosynthesis. In: Raghavendra AS, Sage RF, eds. *C_4 photosynthesis and related CO_2 concentrating mechanisms, Advances in Photosynthesis Vol. 32*. Heidelberg-Berlin: Springer Verlag, 81–108.

Besnard G, Muasya AM, Russier F, Roalson EH, Salamin N, Christin P-A. 2009. Phylogenomics of C_4 photosynthesis in sedges (Cypercaeae): multiple appearances and genetic convergence. *Molecular Biology and Evolution* **26,** 1909–1919.

Bissinger K, Khoshravesh R, Kotrade JP, Oakley J, Sage TL, Sage RF, Hartmann H, Kadereit G. 2014. *Gisekia* (Gisekiaceae): phylogenetic relationships, biogeography, and ecophysiology of a poorly known C_4 lineage in the Caryophyllales. *American Journal of Botany* **101,** 1–11.

Botha CEJ. 1992. Plasmodesmatal distribution, structure and frequency in relation to assimilation in C_3 and C_4 grasses in southern Africa. *Planta* **87,** 348–358.

Bowes G. 2011. Single-cell C_4 photosynthesis in aquatic plants. In: Raghavendra AS, Sage RF, eds. *C_4 photosynthesis and related CO_2 concentrating mechanisms, Advances in Photosynthesis, Vol. 32*. Dordrecht: Springer, 63–80.

Bräutigam A, Weber APM. 2011. Transport processes: connecting the reactions of C_4 photosynthesis. In: Raghavendra AS, Sage RF, eds. *C_4 photosynthesis and related CO_2 concentrating mechanisms, Advances in Photosynthesis, Vol. 32*. Dordrecht: Springer 199–219.

Brown RH, Bouton JH, Rigsby L, Rigler M. 1983. Photosynthesis of grass species differing in carbon-dioxide fixation pathways. VIII. Ultrastructural characteristics of *Panicum* species in the *laxa* group. *Plant Physiology* **71,** 425–431.

Brown RH, Hattersley PW. 1989. Leaf anatomy of C_3–C_4 species as related to evolution of C_4 photosynthesis. *Plant Physiology* **91,** 1543–1550.

Brown WV. 1975. Variations in anatomy, associations, and origins of Kranz tissue. *American Journal of Botany* **62,** 395–402.

Brown WV. 1977. The Kranz syndrome and its subtypes in grass systematics. *Memoirs of the Torrey Botanical Club* **23,** 1–97.

Busch FA, Sage TL, Cousins AB, Sage RF. 2013. C_3 plants enhance rates of photosynthesis by reassimilating photorespired and respired CO_2. *Plant, Cell and Environment* **36,** 200–212.

Christin P-A, Osborne CP, Chatelet DS, Columbus JT, Besnard G, Hodkinson TR, Garrison LM, Vorontsova MS, Edwards EJ. 2013. Anatomical enablers and the evolution of C_4 photosynthesis. *Proceeding of the National Academy of Sciences, USA* **110,** 1381–1386.

Christin P-A, Sage TL, Edwards EJ, Ogburn RM, Khoshravesh R, Sage RF. 2011. Complex evolutionary transitions and the significance of C_3–C_4 intermediate forms of photosynthesis in Molluginaceae. *Evolution* **65,** 643–660.

Christin P-A, Wallace MJ, Clayton H, Edwards EJ, Furbank, Hattersley PW, Sage RF, MacFarlane TD, Ludwig M. 2012. Multiple photosynthetic transitions, polyploidy and lateral gene transfer in the grass subtribe Neurachninae. *Journal of Experimental Botany* **63,** 6297–6308.

Covshoff S, Burgess SJ, Kneřová J, and Kümpers BM. 2014. Getting the most out of natural variation in C_4 photosynthesis. *Photosynthesis Research* **119,** 157–167.

Covshoff S, Furbank RT, Leegood RC, Hibberd JM. 2012. Leaf rolling allows quantification of mRNA abundance in mesophyll cells of sorghum. *Journal of Experimental Botany* **64,** 807–813.

Covshoff S, Hibberd JM. 2012. Integrating C_4 photosynthesis into C_3 crops to increase yield potential. *Current Opinion in Biotechnology* **23,** 209–214.

Dai ZY, Ku MSB, Edwards GE. 1996. Oxygen sensitivity of photosynthesis and photorespiration in different photosynthetic types in the genus *Flaveria*. *Planta* **198,** 563–571.

Dengler NG, Nelson T. 1999. Leaf structure and development in C_4 plants. In: Sage R, Monson R, eds. *C_4 plant biology*. San Diego: Academic Press, 133–172.

Djamali M, Brewer S, Breckle S, Jackson ST. 2012. Climatic determinism in phytogeographic regionalization: A test from the Irano-Turanian region, SW and Central Asia. *Flora* **207,** 237–249.

Edwards EJ, Osborne CP, Stromberg CAE, Smith SA, Consortium CG. 2010. The origins of C_4 grasslands: integrating evolutionary and ecosystem science. *Science* **328,** 587–91.

Edwards GE, Ku MSB. 1987. Biochemistry of C_3–C_4 intermediates. In: MD Hatch, NK Boardman, eds. *Biochemistry of Plants: Photosynthesis, Vol. 14*. San Diego: Academic Press 275–325.

Edwards GE, Voznesenskaya EV. 2011. Kranz forms and single cell C_4 in terrestrial plants. In: Raghavendra AS, Sage RF, eds. *C_4 photosynthesis and related CO_2 concentrating mechanisms, Advances in Photosynthesis Vol. 32*. Heidelberg-Berlin: Springer Verlag, 29–61.

Engelmann S, Bläsing OE, Gowik U, Svensson P, Westhoff P. 2003. Molecular evolution of C_4 phosphoenolpyruvate carboxylase in the genus *Flaveria* - a gradual increase from C_3 to C_4 characteristics. *Planta* **217,** 717–725.

Evert RF, Eschrich W, Heyser W. 1977. Distribution and structure of the plasmodesmata in mesophyll and bundle-sheath cells of *Zea mays* L. *Planta* **136,** 77–89.

Feodorova TA, Voznesenskaya EV, Edwards GE, Roalson EH. 2010. Biogeographic patterns of diversification and the origins of C_4 in *Cleome* (Cleomaceae). *Systematic Botany* **35,** 811–826.

Fouracre JP, Ando S, Langdale JA. 2014. Cracking the Kranz enigma with systems biology. *Journal of Experimental Botany* **65,** 3327–3339.

Freitag H, Kadereit G. 2013. C_3 and C_4 leaf anatomy types in Camphorosmeae (Camphorosmoideae, Chenopodiaceae). *Plant Systematics and Evolution* doi 10.1007/s00606-013-0912-9.

Frohlich MW. 1978. *Systematics of Heliotropium section Orthostachys in Mexico*. PhD thesis, Cambridge, Massachusetts: Harvard University.

Furbank RT. 2011. Evolution of C_4 photosynthetic mechanism: are there really three C_4 acid decarboxylation types? *Journal of Experimental Botany* **62,** 3103–3108.

Gowik U, Westhoff P. 2011. C_4-phosphoenolpyruvate carboxylase. In: Raghavendra AS, Sage RF, eds. *C4 photosynthesis and related CO2 concentrating mechanisms, Advances in Photosynthesis, Vol. 32*. Dordrecht, The Netherlands: Springer, 257–275.

Grass Phylogeny Working Group II. 2012. New grass phylogeny resolves deep evolutionary relationships and discovers C_4 origins. *New Phytologist* **193,** 304–312.

Griffiths H, Weller G, Toy LF, Dennis RJ. 2013. You're so vein: bundle sheath physiology, phylogeny and evolution in C_3 and C_4 plants. *Plant, Cell and Environment* **36,** 249–261.

Haberlandt G. 1914. *Physiological Plant Anatomy*. Macmillan, London.

Hatch MD. 1987. C_4 photosynthesis: a unique blend of modified biochemistry, anatomy and ultrastructure. *Biochimica et Biophysica Acta* **895,** 81–106.

Hattersley PW. 1984. Characterization of C_4 type leaf anatomy in grasses (Poaceae). Mesophyll:bundles sheath area ratios. *Annals of Botany* **53,** 163–179.

Hattersley PW, Browning AJ. 1981. Occurrence of the suberized lamella in leaves of grasses of different photosynthetic types. I. In parenchymatous bundle sheaths and PCR (“Kranz”) sheaths. *Protoplasma* **109,** 371–401.

Hattersley PW, Watson L. 1992. Diversification of photosynthesis. In: Chapman GP, ed. *Grass evolution and domestication*. London: Academic Press, 38–116.

Hattersley PW, Watson L, Johnston CR. 1982. Remarkable leaf anatomical variations in *Neurachne* and its allies (Poaceae) in relation to C_3 and C_4 photosynthesis. *Botanical Journal of the Linnean Society* **84,** 265–272.

Hattersley PW, Wong SC, Perry S, Roksandic Z. 1986. Comparative ultrastructure and gas-exchange characteristics of the C_3–C_4 intermediate *Neurachne minor* S. T. Blake (Poaceae). *Plant, Cell and Environment* **9,** 217–233.

Heckmann D, Schulze S, Denton A, Gowik U, Westhoff P, Andreas PM, Lercher MJ. 2013. Predicting C_4 photosynthesis evolution: modular, individually adaptive steps on a Mount Fuji fitness landscape. *Cell* **153,** 1579–1588.

Holaday AS, Black CC. 1981. Comparative characterization of phosphoenolpyruvate carboxylase in C_3, C_4 and C_3–C_4 intermediate *Panicum* species. *Plant Physiology* **67,** 330–334.

Holaday AS, Chollet R. 1984. Photosynthetic/photorespiratory characteristics of C_3–C_4 intermediate species. *Photosynthesis Research* **5,** 307–323.exas

Holaday AS, Lee KW, Chollet R. 1984. C_3–C_4 intermediate species in the genus *Flaveria*: leaf anatomy, ultrastructure, and the effect of O_2 on the CO_2 compensation concentration. *Planta* **160,** 25–32.

Hylton CM, Rawsthorne S, Smith AM, Jones DA, Woolhouse HW. 1988. Glycine decarboxylase is confined to the bundle sheath cells of leaves of C_3–C_4 intermediate species. *Planta* **175,** 452–459.

Kadereit G, Ackerly D, Pirie MD. 2012. A broader model for C_4 photosynthesis evolution in plants inferred from the goosefoot family (Chenopodiaceae *s.s*.). *Proceeding of the Royal Society, Biological Science* **279,** 3304–3311.

Kadereit G, Freitag H. 2011. Molecular phylogeny of Camphorosmeae (Camphorosmoideae, Chenopodiaceae): Implications for biogeography, evolution of C_4 photosynthesis and taxonomy. *Taxon* **60,** 51–78.

Keeley JE. 1990. Photosynthetic pathways in freshwater aquatic plants. *Trends in Ecology and Evolution* **5,** 330–333.

Kennedy RA, Eastburn KL, Jensen KG. 1980. C_3–C_4 photosynthesis in the genus *Mollugo*: structure, physiology and evolution of intermediate characteristics. *American Journal of Botany* **67,** 1207–1217.

Khoshravesh R, Akhani H, Sage TL, Nordenstam B, Sage RF. 2012. Phylogeny and photosynthetic pathway distribution in *Anticharis* Endl. (Scrophulariaceae). *Journal of Experimental Botany* **63,** 5645–5658.

Kocacinar F, McKown AD, Sage TL, Sage RF. 2008. Photosynthetic pathway influences xylem structure and function in *Flaveria* (Asteraceae). *Plant, Cell and Environment* **31,** 1363–1376.

Koteyeva NK, Voznesenskaya EV, Roalson EH, Edwards GE. 2011. Diversity in forms of C_4 in the genus *Cleome* (Cleomaceae). *Annals of Botany* **107,** 269–283.

Ku MSB, Wu J, Dai Z, Scott RA, Chu C, Edwards GE. 1991. Photosynthetic and photorespiratory characteristics of *Flaveria* species. *Plant Physiology* **96,** 518–528.

Laetsch WM. 1974. The C_4 syndrome: a structural analysis. *Annual Review Plant Physiology* **25,** 27–52.

Ludwig M. 2011. The molecular evolution of β-carbonic anhydrase in *Flaveria*. *Journal of Experimental Botany* **62,** 3071–3081.

Ludwig M. 2013. Evolution of the C_4 photosynthetic pathway: events at the cellular and molecular levels. *Photosynthesis Research* **117,** 147–161.

Marshall DM, Muhaidat R, Brown NJ, Liu Z, Griffiths H, Sage RF, Hibberd JM. 2007. *Cleome*, a genus closely related to *Arabidopsis*, contains species spanning a developmental progression from C_3 to C_4 photosynthesis. *Plant Journal* **51,** 886–896.

McKown AD, Dengler NG. 2007. Key innovations in the evolution of Kranz anatomy and C_4 vein pattern in *Flaveria* (Asteraceae). *American Journal of Botany* **94,** 382–399.

McKown AD, Dengler NG. 2009. Shifts in leaf vein density through accelerated vein formation in C_4 *Flaveria* (Asteraceae). *Annals of Botany* **104,** 1085–1098.

McKown AD, Moncalvo JM, Dengler NG. 2005. Phylogeny of *Flaveria* (Asteraceae) and inference of C_4 photosynthesis evolution. *American Journal of Botany* **92,** 1911–1928.

Mertz RA, Brutnell TP. 2014. Bundle sheath suberization in grass leaves: multiple barriers to characterization. *Journal of Experimental Botany* **65,** 3371–3380.

Metcalfe CR, Chalk L. 1979. *Anatomy of the Dicotyledons, Second Edition, Volume 1: Systematic Anatomy of the Leaf and Stem*. Oxford: Oxford University Press.

Monson RK. 1989. On the evolutionary pathways resulting in C_4 photosynthesis and Crassulacean acid metabolism. *Advances in Ecological Research* **19,** 57–110.

Monson RK. 1999. The origins of C_4 genes and evolutionary pattern in the C_4 metabolic phenotype. In: Sage R, Monson R, eds. *C4 Plant Biology*. San Diego: Academic Press, 337–410.

Monson RK, Edwards GE, Ku MSB. 1984. C_3–C_4 intermediate photosynthesis in plants. *Bioscience* **34,** 563–571.

Monson RK, Moore BD. 1989. On the significance of C_3–C_4 intermediate photosynthesis to the evolution of C_4 photosynthesis. *Plant, Cell and Environment* **12,** 689–699.

Monson RK, Rawsthorne S. 2000. Carbon dioxide assimilation in C_3–C_4 intermediate plants. In: Leegood R, Sharkey T, Von Caemmerer S, eds. *Photosynthesis: physiology and metabolism. Advances in Photosynthesis*, Vol. **9**. Dordrecht: Kluwer Academic Press, 533–550.

Monson RK, Schuster WS, Ku MSB. 1987. Photosynthesis in *Flaveria brownii* A.M. Powell, a C_4-like C_3–C_4 intermediate. *Plant Physiology* **85,** 1063–1067.

Monson RK, Teeri JA, Ku MSB, Gurevitch J, Mets LJ, Dudley S. 1988 Carbon-isotope discrimination by leaves of *Flaveria* species exhibiting different amounts of C_3- and C_4-cycle cofunction. *Planta* **174,** 145–151.

Moore BD, Franceschi VR, Cheng SH, Wu JR, Ku MSB. 1987a. Photosynthetic characteristics of the C_3–C_4 intermediate *Parthenium hysterophorus*. *Plant Physiology* **85,** 978–983.

Moore BD, Ku MSB, Edwards GE. 1987b. C_4 photosynthesis and light-dependent accumulation of inorganic carbon in leaves of C_3–C_4 and C_4 *Flaveria* species. *Australian Journal of Plant Physiology* **14,** 657–668.

Moore BD, Ku MSB, Edwards GE. 1989. Expression of C_4-like photosynthesis in several species of *Flaveria*. *Plant, Cell and Environment* **12,** 541–549.

Morgan JA, Brown RH. 1980. Photosynthesis in grass species differing in carbon dioxide fixation pathways. III. Oxygen response and enzyme activities of the *Laxa* groups of *Panicum*. *Plant Physiology* **65,** 156–159.

Muhaidat R, Sage RF, Dengler NG. 2007. Diversity of Kranz anatomy and biochemistry in C_4 eudicots. *American Journal of Botany* **94,** 362–381.

Muhaidat R, Sage TL, Frohlich MW, Dengler NG, Sage RF. 2011. Characterization of C_3–C_4 intermediate species in the genus *Heliotropium* L. (Boraginaceae): anatomy, ultrastructure and enzyme activity. *Plant, Cell and Environment* **34,** 1723–1736.

Oakley JC, Sultmanis S, Stinson CR, Sage TL, Sage RF. 2014. Comparative studies of C_3 and C_4 *Atriplex* hybrids in the genomics era: physiological assessments. *Journal of Experimental Botany* **65,** 3637–3647.

Ocampo G, Koteyeva NK, Voznesenskaya EV, Edwards GE, Sage TL, Sage RF, Columbus JT. 2013. Evolution of leaf anatomy and photosynthetic pathways in Portulacaeae. *American Journal of Botany* **100,** 2388–2402.

Osborne CP, Sack L. 2012. Evolution of C_4 plants: a new hypothesis for an interaction of CO_2 and water relations mediated by plant hydraulics. *Philosophical Transactions of the Royal Society, Biological Science* **367,** 583–600.

Pyankov VI, Voznesenskaya EV, Kuzmin AN, Ku MSB, Ganko E, Franceschi VR, Black CC, Edwards GE. 2000. Occurrence of C_3 and C_4 photosynthesis in cotyledons and leaves of *Salsola* species (Chenopodiaceae). *Photosynthesis Research* **63,** 69–84.

Rajendrudu G, Prasad JSR, Das VSR. 1986. C_3–C_4 intermediate species in *Alternanthera* (Amaranthaceae) - leaf anatomy, CO_2 compensation point, net CO_2 exchange and activities of photosynthetic enzymes. *Plant Physiology* **80,** 409–414.

Rawsthorne S. 1992. C_3–C_4 intermediate photosynthesis: linking physiology to gene expression. *Plant Journal* **2,** 267–274.

Rawsthorne S, Bauwe H. 1998. C_3–C_4 intermediate photosynthesis. In: Raghavendra AS, eds. *Photosynthesis. A comprehensive treatise*. Cambridge: Cambridge University Press, 150–162.

Rawsthorne S, Hylton CM, Smith AM, Woolhouse HW. 1988. Photorespiratory metabolism and immunogold localization of photorespiratory enzymes in leaves of C_3 and C_3–C_4 intermediate species of *Moricandia*. *Planta* **173,** 298–308.

Roalson EH. 2011. C_4 photosynthesis origins in the monocots: a review and reanalysis. In: Raghavendra AS, Sage RF, eds. *C_4 photosynthesis and related CO_2 concentrating mechanisms, Advances in Photosynthesis Vol. 32*. Dordrecht: Springer, 319–338.

Roalson EH, Hinchliff CE, Trevisan R, da Silva CRM. 2010. Phylogenetic relationships in *Eleocharis* (Cyperaceae): C_4 photosynthesis origins and patterns of diversification in the spikerushes. *Systematic Botany* **35,** 257–271.

Roth-Nebelsick A, Uhl D, Mosbrugger V, Kerp H. 2001. Evolution and function of leaf venation architecture: a review. *Annals of Botany* **87,** 553–566.

Sabale AB, Bhosale LJ. 1984. C_3–C_4 photosynthesis in *Bougainvillea* cv. Palmer, Mary. *Photosynthetica* **18,** 84–89.

Sage RF. 2001. Environmental and evolutionary preconditions for the origin and diversification of the C_4 photosynthesis syndrome. *Plant Biology* **3,** 202–213.

Sage RF. 2002. Are CAM and C_4 photosynthesis incompatible? *Australian Journal of Plant Physiology* **29,** 775–785.

Sage RF. 2004. The evolution of C_4 photosynthesis. *New Phytologist* **161,** 341–370.

Sage RF. 2013. Photorespiratory compensation: a driver for biological diversity. *Plant Biology* **15,** 624–638.

Sage TL, Busch FA, Johnson DC, Friesen PC, Stinson CR, Stata M, Sultmanis S, Rahman BA, Rawsthorne S, Sage RF. 2013. Initial events during the evolution of C_4 photosynthesis in C_3 species of *Flaveria*. *Plant Physiology* **163,** 1266–1276.

Sage RF, Christin P A, Edwards E J. 2011*a*. The C_4 plant lineages of planet Earth. *Journal of Experimental Botany* **62,** 3155–3169.

Sage RF, Li MR, Monson RK. 1999. The taxonomic distribution of C4 photosynthesis. In: Sage R, Monson RK, eds. *C_4 plant Biology*. San Diego: Academic Press, 551–584.

Sage RF, Sage TL, Kocacinar F. 2012. Photorespiration and the evolution of C_4 photosynthesis. *Annual Review of Plant Biology* **63,** 19–47.

Sage RF, Sage TL, Pearcy RW, Borsch T. 2007. The taxonomic distribution of C_4 photosynthesis in Amaranthaceae s*ensu stricto*. *American Journal of Botany* **94,** 1992–2003.

Sage TL, Sage RF, Vogan PJ, Rahman B, Johnson DC, Oakley JC, Heckel MA. 2011*b*. The occurrence of C_2 photosynthesis in *Euphorbia* subgenus *Chamaesyce* (Euphorbiaceae). *Journal of Experimental Botany* **62,** 3183–3195.

Schulze S, Mallmann J, Burscheidt J, Koczor M, Streubel M, Bauwe H, Gowik U, Westhoff P. 2013. Evolution of C_4 photosynthesis in the genus *Flaveria*: Establishment of a photorespiratory CO_2 pump. *The Plant Cell* **25,** 2522–2535.

Slewinski TL. 2013. Using evolution as a guide to engineer Kranz-type C_4 photosynthesis. *Frontiers in Plant Science* **4,** 1–13.

Smith JAC, Winter K. 1996. Taxonomic distribution of crassulacean acid metabolism. In: Winter K, Smith JAC, eds. *Crassulacean acid metabolism: biochemistry, ecophysiology and evolution*. Berlin: Springer-Verlag, 427–436.

Soros CL, Dengler NG. 2001. Ontogenetic derivation and cell differentiation in photosynthetic tissues of C_3 and C_4 species of the Cyperaceae. *American Journal of Botany* **88,** 992–1005.

Stata M, Sage TL, Rennie TD, Khoshravesh R, Sultmanis S, Khaikin Y, Ludwig M, Sage RF. 2014 Mesophyll cells of C_4 plants have fewer chloroplasts than those of closely related C_3 plants. *Plant Cell and Environment*. doi: 10.1111/pce.12331.

Ueno O, Bang SW, Wada Y, Kobayashi N, Kaneko R, Kaneko Y, Matsuzawa Y. 2007. Inheritance of C3–C4 intermediate photosynthesis in reciprocal hybrids between *Moricandia arvensis* (C_3–C_4) and *Brassica oleracea* (C_3) that differ in genome constitution. *Plant Production Science* **10,** 68–79.

Ueno O, Bang SW, Wada Y, Kondo A, Ishihara K, Kaneko Y, Matsuzawa Y. 2003. Structural and biochemical dissection of photorespiration in hybrids differing in genome constitution between *Diplotaxis tenuifolia* (C_3–C_4) and Radish (C_3). *Plant Physiology* **132,** 1550–1559.

Ueno O, Wada Y, Wakai M, Bang SW. 2006. Evidence from photosynthetic characteristics for the hybrid origin of *Diplotaxis muralis* from a C_3–C_4 intermediate and a C_3 species. *Plant Biology* **8,** 253–259.

Vogan PJ, Frohlich MW, Sage RF. 2007. The functional significance of C_3–C_4 intermediate traits in *Heliotropium* L. (Boraginaceae): gas exchange perspective. *Plant, Cell and Environment* **30,** 1337–1345.

Vogan PJ, Sage RF. 2011. Water-use efficiency and nitrogen-use efficiency of C_3–C_4 intermediate species of *Flaveria* Juss. (Asteraceae). *Plant, Cell and Environment* **34,** 1415–1430.

von Caemmerer S. 1989. A model of photosynthetic CO_2 assimilation and carbon-isotope discrimination in leaves of certain C_3–C_4 intermediates. *Planta* **178,** 463–474.

von Caemmerer SV. 2000. *Biochemical models of leaf photosynthesis*. CSIRO Publishing, Australia.

von Caemmerer C, Furbank R. 2003. The C_4 pathway: an efficient CO_2 pump. *Photosynthesis Research* **77,** 191–207.

Voznesenskaya EV, Artyusheva EG, Franceschi VR, Pyankov VI, Kiirats O, Ku MSB, Edwards GE. 2001. *Salsola arbusculiformis*, a C_3–C_4 Intermediate in Salsoleae (Chenopodiaceae). *Annals of Botany* **88,** 337–348.

Voznesenskaya EV, Franceschi VR, Pyankov VI, Edwards GE. 1999. Anatomy, chloroplast structure and compartmentation of enzymes relative to photosynthetic mechanisms in leaves and cotyledons of species in the tribe Salsoleae (Chenopodiaceae). *Journal of Experimental Botany* **50,** 1779–1795.

Voznesenskaya EV, Gamaley YV. 1986. The ultrastructural characteristics of leaf types with Kranz-anatomy. *Botanicheskii Zhurnal* **71,** 1291–1307 (In Russian).

Voznesenskaya EV, Koteyeva NK, Akhani H, Roalson EH, Edwards GE. 2013. Structural and physiological analyses in Salsoleae (Chenopodiaceae) indicate multiple transitions among C_3, intermediate and C_4 photosynthesis. *Journal of Experimental Botany* **64,** 3583–3604.

Voznesenskaya EV, Koteyeva NK, Chuong SDX, Ivanova AN, Barroca J, Craven LA, Edwards GE. 2007. Physiological, anatomical and biochemical characterisation of photosynthetic types in genus *Cleome* (Cleomaceae). *Functional Plant Biology* **34,** 247–267.

Voznesenskaya EV, Koteyeva NK, Edwards GE, Ocampo G. 2010. Revealing diversity in structural and biochemical forms of C_4 photosynthesis and a C_3–C_4 intermediate in genus *Portulaca* L. (Portulacaceae). *Journal of Experimental Botany* **61,** 3647–3662.

Williams BP, Johnston IG, Covshoff S, Hibberd JM. 2013. Phenotypic landscape inference reveals multiple evolutionary paths to C_4 photosynthesis. *eLife* **2,** e00961.

Yang Y, Berry PE. 2011. Phylogenetics of the Chamaesyce clade (*Euphorbia*, Euphorbiaceae): reticulate evolution and long-distance dispersal in a prominent C_4 lineage. *American Journal of Botany* **98,** 1486–1503.